Vertical profiles of activated ClO and ozone loss in the Arctic vortex in January and March 2000: In situ observations and model simulations

Bärbel Vogel,[1] Rolf Müller,[1] Terry Deshler,[2] Jens-Uwe Grooß,[1] Juha Karhu,[3] Daniel S. McKenna,[4] Melanie Müller,[5] Darin Toohey,[6] Geoffrey C. Toon,[7] and Fred Stroh[1]

Received 24 May 2002; revised 11 June 2003; accepted 14 July 2003; published 26 November 2003.

[1] In situ observations of ClO mixing ratios obtained from a balloonborne instrument launched in Kiruna on 27 January 2000 and on 1 March 2000 are presented. ClO mixing ratios and quasi-simultaneously observed ozone loss are compared to model simulations performed with the Chemical Lagrangian Model of the Stratosphere (CLaMS). ClO mixing ratios are simulated initializing the model simulations for early winter conditions. Sensitivity studies are performed to explore the impact of the surface area of the background aerosol, of denitrification, and of the recently reported kinetics of the ClO self-reaction [*Bloss et al.*, 2001] on simulated ClO. For 27 January 2000, model simulations agree with rate constants reported by *Bloss et al.* [2001], whereas for 1 March 2000 simulations employing rate constants reported by *Bloss et al.* [2001] and by *Sander et al.* [2000] reproduce the ClO measurements. The impact of uncertainties arising from accumulated errors along the calculated backward trajectories and uncertainties within temperatures derived from the UK Met Office are also studied. For both flights, simulated ClO show a good overall agreement with measured ClO within uncertainties arising from accumulated errors along air parcel histories. We find a layer of low ClO mixing ratios < 100 pptv between 600 and 620 K for the flight on 27 January 2000 and between 525 and 550 K on 1 March 2000. For this layer, measured ClO is substantially lower than simulated ClO. Potential causes are discussed, but the discrepancy remains unexplained at present. Furthermore, for 1 March 2000, an overall agreement is found between model simulations and measurements by the HALOE instrument of HCl and NO_x (=NO + NO_2) for all altitudes considered. We conclude that denitrification occurred up to a potential temperature of ≈550 K (≈24 km altitude) on 1 March 2000. Finally, model simulations show that between late January and 1 March, a significant ozone loss of about 0.8–1.8 ppmv is derived between 425 and 490 K of potential temperature in agreement with measured ozone loss and correlated with the enhanced ClO. For 1 March 2000, 77 ± 10 DU is obtained as an estimate of the loss in column ozone. *INDEX TERMS:* 0317 Atmospheric Composition and Structure: Chemical kinetic and photochemical properties; 0394 Atmospheric Composition and Structure: Instruments and techniques; 0399 Atmospheric Composition and Structure: General or miscellaneous; *KEYWORDS:* chlorine monoxide (ClO), chlorine activation, ozone loss, TRIPLE, CLaMS, THESEO 2000

Citation: Vogel, B., R. Müller, T. Deshler, J.-U. Grooß, J. Karhu, D. S. McKenna, M. Müller, D. Toohey, G. C. Toon, and F. Stroh, Vertical profiles of activated ClO and ozone loss in the Arctic vortex in January and March 2000: In situ observations and model simulations, *J. Geophys. Res.*, *108*(D22), 8334, doi:10.1029/2002JD002564, 2003.

[1]Institute for Stratospheric Research (ICG-I), Research Center Jülich, Jülich, Germany.
[2]Department of Atmospheric Science, University of Wyoming, Laramie, Wyoming, USA.
[3]Finnish Meteorological Institute, Sodankylä, Finland.
[4]National Center for Atmospheric Research, Boulder, Colorado, USA.
[5]Institute for Meteorology, University of Frankfurt, Frankfurt, Germany.
[6]Program in Atmospheric and Oceanic Sciences, University of Colorado, Boulder, Colorado, USA.
[7]Jet Propulsion Laboratory, California Institute of Technology, Pasadena, California, USA.

0148-0227/03/2002JD002564$09.00

1. Introduction

[2] Chlorine monoxide (ClO) plays a key role in stratospheric ozone loss processes. The observed ozone depletion in the Arctic vortex is caused by catalytic cycles involving the halogen radicals ClO and BrO similar to the ozone depletion observed in the Antarctic vortex [*Solomon*, 1990]. However, there are still open questions regarding the quantitative understanding of Arctic polar ozone chemistry as has been revealed by apparent discrepancies found in comparisons of observed and simulated ozone losses [e.g., *Hansen et al.*, 1997; *Becker et al.*, 1998; *Deniel et al.*, 1998;

Goutail et al., 1999; *Woyke et al.*, 1999; *Kilbane-Dawe et al.*, 2001]. A prerequisite for the reliable calculation of halogen-induced ozone loss rates is the understanding of the seasonal behavior of ClO as a function of altitude.

[3] Contradictory analyses can be found by utilizing direct measurements of ClO for ozone loss calculations. Model studies for the Antarctic vortex found no evidence of unknown halogen chemistry, thus supporting the current theories of ozone depletion chemistry [e.g., *Anderson et al.*, 1991; *Wu and Dessler*, 2001]. In contrast, in a similar study for the Arctic polar vortex the observed ozone loss in early winter is underestimated, although observed ClO mixing ratios are well reproduced by the model [*Woyke et al.*, 1999].

[4] In winter 1999/2000 the SOLVE/THESEO 2000 campaign was conducted with the aim of studying Arctic ozone loss in great detail [*Newman et al.*, 2002]. The Arctic winter 1999/2000 is characterized by a stable stratospheric circulation and by very low temperatures that cause extensive occurrence of polar stratospheric clouds (PSCs) [e.g., *Manney and Sabutis*, 2000; *Bevilacqua et al.*, 2002]. Heterogeneous reactions on the surface of PSCs led to the formation of active chlorine (ClO, Cl_2O_2) from the reservoir species HCl and $ClONO_2$, initiating chemical ozone depletion in the presence of sunlight. During this winter strong widespread denitrification and also some dehydration due to sedimentation of large PSC particles was observed [e.g., *Fahey et al.*, 2001; *Schiller et al.*, 2002; *Popp et al.*, 2001]. By the end of the winter, these chemical processes led to a 70% reduction of ozone for a ≈1 km thick layer of the lower stratosphere [*Rex et al.*, 2002; *Müller et al.*, 2002]. By the end of March 2000 up to 30% of the Arctic ozone column had been chemically depleted [*Sinnhuber et al.*, 2000].

[5] Here we investigate the extent to which the observed vertical distribution of ClO and the simultaneously observed ozone loss can be quantitatively reproduced in models for the Arctic winter 1999/2000. We study this question employing two balloonborne in situ measurements of ClO: one to study the period of lowest temperatures and of maximum chlorine activation in early winter and a second to study the period of chlorine recovery and maximum ozone loss in late winter. ClO in situ measurements taken on board the TRIPLE balloon gondola launched on 27 January 2000 and on 1 March 2000 from Esrange near Kiruna, Sweden, are presented. Between an altitude of 12 and 26 km ClO mixing ratios were measured on 27 January 2000 at sunset and on 1 March 2000 at sunrise. We compare these ClO observations and the quasi-simultaneously observed ozone loss with results of model simulations performed by the box model version of the Chemical Lagrangian Model of the Stratosphere (CLaMS) [*McKenna et al.*, 2002a, 2002b].

2. Observations

[6] Within the framework of the THESEO 2000 campaign the multi-instrument payload TRIPLE was launched on 27 January 2000 and on 1 March 2000 from Esrange (67.5°N, 21.0°E) near Kiruna, Sweden. TRIPLE consists of the Jülich ClO/BrO in situ instrument, the cryogenic whole air sampler of the University of Frankfurt for observation of long-lived tracers [*Schmidt et al.*, 1987], and the Jülich Fast In-situ Stratospheric Hygrometer (FISH) [*Schiller et al.*, 2002]. On both flights, an ECC ozonesonde (electrochemical concentration cell) was part of the payload but on both occasions the signal was jammed and no O_3 data could be obtained. Other quasi-simultaneous measurements of ozone were therefore employed here for the analysis of ozone loss (see below).

2.1. Measurement Techniques

[7] The new Jülich ClO/BrO in situ instrument was developed as part of a collaboration with the University of California at Irvine. A prototype instrument was flown in Kiruna in February 1995 [*Pierson et al.*, 1999; *Woyke et al.*, 1999].

[8] The instrument employs the well-established chemical-conversion resonance-fluorescence technique [*Brune et al.*, 1989]. Briefly, stratospheric air is pulled through a flow tube by a modified roots pump, and NO is periodically added at the inlet. The addition of NO converts ClO to chlorine atoms, which are detected downstream by atomic resonance fluorescence at 118.9 nm. The raw signal consists of the background signal due to Rayleigh scatter and an additional Cl resonance fluorescence signal during NO addition cycles. The chlorine calibration is performed in the laboratory before and after the flight with Cl mixing ratios quantified through absorption measurements of the 118.9 nm doublet [*Anderson et al.*, 1991; *Toohey et al.*, 1993]. A chemical model with currently accepted reaction rates [*DeMore et al.*, 1997] is employed to calculate the ClO mixing ratios from the measured Cl abundance, pressure, temperature, and ozone mixing ratios. The Jülich ClO/BrO in situ instrument is equipped with three detection axes stacked in the order ClO, BrO, and ClO. This enables a rigorous check of the ClO to Cl conversion kinetics by comparing the results of the two Cl detection axes with the model results. Here we generally find a good agreement pointing to the validity of the method employed. The overall accuracy of the ClO measurement is usually 20%, but due to a temporary leakage of the NO injection device during the January flight the accuracy was reduced to 35% during ascent and 25% during descent. For measured ClO mixing ratios below 50 pptv we deduced an error of ±10 pptv.

[9] Air samples taken by the cryogenic whole air sampler were analyzed in the laboratory by gas chromatography to determine the mixing ratios of different long-lived trace gases like N_2O and CH_4, as well as various CFCs accounting for ≈95% of organic chlorine in the form of source gases, from which the amount of total inorganic chlorine Cl_y could be inferred [*Schmidt et al.*, 1994; *Engel et al.*, 1997].

2.2. Flight Profiles

[10] To study in detail the sunrise and sunset evolution of the halogen oxide mixing ratios a new type of flight profile was employed (Figure 1). On the basis of the analyzed potential vorticity (PV) at the location of the balloon flight, both flights were undertaken well within inside the Arctic polar vortex (e.g., PV $\geq$ 30 PVU at Θ = 475 K and PV $\geq$ 75 PVU at Θ = 550 K).

[11] On 27 January 2000 the balloon was launched at ≈11:00 UT, reached a maximum altitude of 20 hPa (≈25 km), descended to a plateau at 37 hPa (≈22 km) and floated at this altitude into the sunset between 92° and 98° solar zenith angle (SZA), thus measuring the decline of

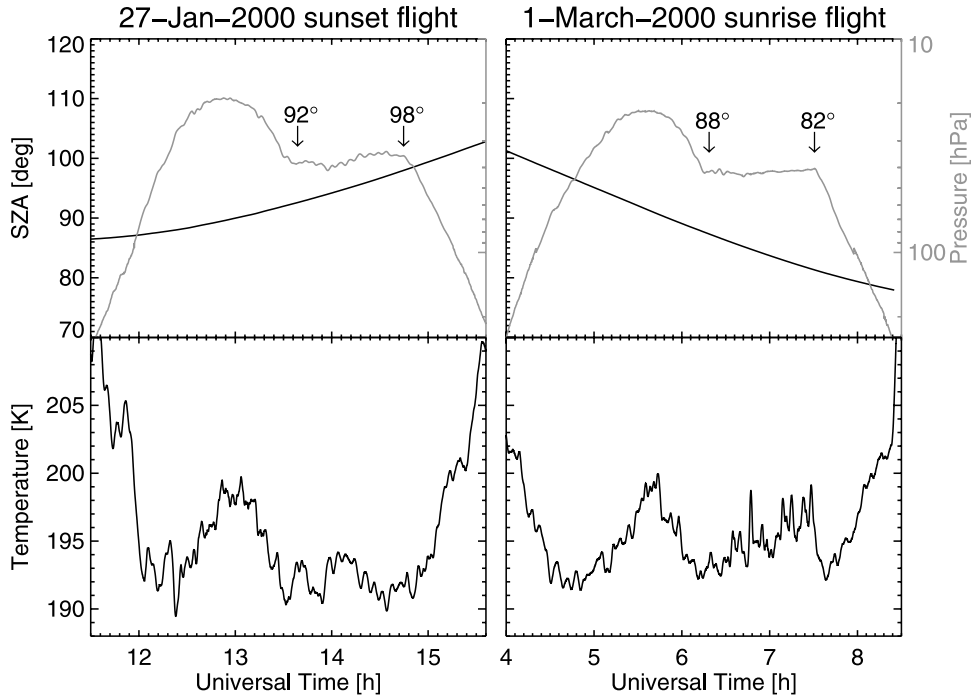

Figure 1. Meteorological parameters for the flights of the TRIPLE gondola on (left) 27 January 2000 and on (right) 1 March 2000 as a function of UT time. (top) Pressure (gray line) and solar zenith angle (SZA) (black line). Beginning and end of the float is marked by arrows; the corresponding solar zenith angles are also noted. (bottom) Temperature (black line).

the ClO mixing ratio within this air mass. The final descent took place during darkness (SZA $\geq$ 98°).

[12] On 1 March 2000 a similar flight profile was flown except that the float was conducted during sunrise. The balloon was launched during the night at ≈4:00 UT, a maximum altitude of 22 hPa (≈24 km) was reached and the float took place at approximately 42 hPa (≈21 km) in the 88° and 82° SZA interval. The final descent took place in daylight.

[13] Altitude profiles of ClO mixing ratios were measured during darkness, twilight, and in daylight. ClO mixing ratios were also measured within a particular air mass at one particular level of potential temperature to observe the change of ClO mixing ratios as a function of SZA during sunset or sunrise (B. Vogel et al., Diurnal variation of ClO and impact of mesoscale PSCs in the Arctic polar vortex 2000: In situ observations and model simulations, submitted to *Journal of Geophyscial Research*, 2002).

2.3. ClO and O_3 Measurements

[14] The two ClO vertical profiles measured by the TRIPLE balloon payload in winter 1999/2000 are shown in Figure 2. On 27 January a ClO daylight profile was measured, with ClO peak values of 1300 pptv at around 540 K potential temperature. On 1 March an activated ClO layer was measured around 500 K potential temperature with enhanced ClO mixing ratios up to 2100 pptv. In addition, ozone mixing ratios are shown in Figure 2 which were measured quasi-simultaneously by an ozonesonde on board the HALOZ payload launched one hour after TRIPLE on 27 January 2000 from Esrange and measured by an ozonesonde launched on 1 March 2000 from Sodankylä, northern Finland (67.4°N, 26.6°E, ≈200 km eastern of Kiruna) at about 11:15 UT (5 hours after TRIPLE).

3. Model Simulations

3.1. Model Description

[15] For the model simulations we used the Chemical Lagrangian Model of the Stratosphere (CLaMS). The model is described in detail by *McKenna et al.* [2002a, 2002b]. It simulates both the chemistry of multiple air parcels and their transport. Here CLaMS is used as a photochemical box model. The chemistry scheme includes full chlorine and bromine chemistry, 36 chemical species and 112 chemical reactions (containing 24 photolysis and 11 heterogeneous reactions). The model employs the ASAD package for the integration of the set of coupled differential equations describing the chemistry [*Carver et al.*, 1997]. Several solvers are available for integration: a standard routine employing the family concept and explicit stiff solvers [*Carver and Scott*, 2000]. All calculations presented here were conducted with the stiff solver SVODE. Photolysis frequencies are calculated by a scheme that solves the radiative transfer equation in spherical geometry [*Lary and Pyle*, 1991; *Becker et al.*, 2000]. The absorption cross sections and reaction rate constants are taken from current recommendations [*Sander et al.*, 2000].

[16] The heterogeneous reaction rates and the microphysics of liquid and solid aerosol are calculated using the scheme developed by [*Carslaw et al.*, 1995]. The particle phases considered in the heterogeneous reaction schemes are liquid ternary $H_2SO_4/HNO_3/H_2O$ solutions, solid sulfuric acid tetrahydrate (SAT), nitric acid trihydrate (NAT), and

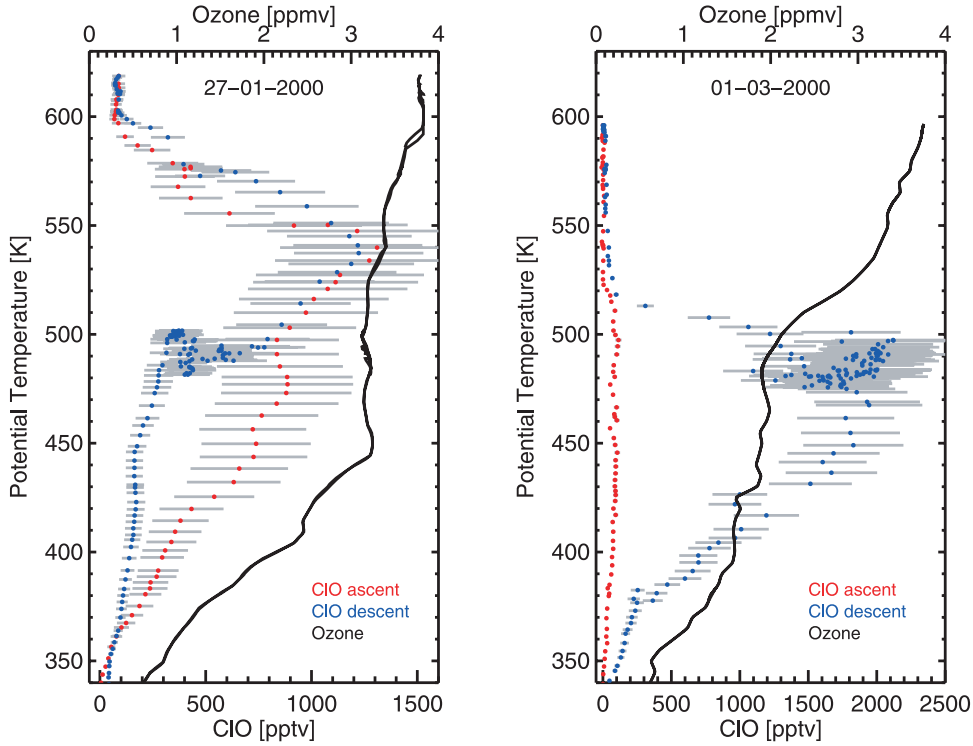

Figure 2. (left) Measured ClO mixing ratios as a function of the potential temperature of the TRIPLE flight on 27 January 2000. During the ascent a ClO daylight profile (red dots) with a maximum ClO mixing ratio of 1300 pptv at 550 K was observed. During the descent (blue dots) the balloon floated at a constant potential temperature level of 490 K into the sunset. The ClO mixing ratios decrease to 300 pptv during sunset. The 1 σ accuracy for the ClO measurement is 35% on ascent and 25% on descent (gray bars). In addition, O_3 mixing ratios are plotted (black line), which were measured quasi-simultaneously by the HALOZ payload launched from Esrange one hour after TRIPLE on 27 January 2000. (right) Measured ClO mixing ratios as a function of the potential temperature of the TRIPLE flight on 1 March 2000: During the ascent in darkness (red dots) only low ClO mixing ratios up to 100 pptv were observed. The ClO daylight profile is observed on descent (blue dots). During descent (blue dots) the balloon floated at a constant potential temperature level of 490 K into the sunrise. The 1 σ accuracy for this ClO measurement is approximately 20% (gray bars). In addition, O_3 mixing ratios are plotted (black line) measured quasi-simultaneously by an ozonesonde launched on 1 March 2000 from Sodankylä, northern Finland (67.4°N, 26.6°E) at about 11:15 UT.

water ice particles. The different particle types can exist alone or in a mixture of several different particle types. For our simulations we used the following standard case: a mixture of SAT, NAT, ternary solutions, and ice particles with a supersaturation of 10 required for NAT formation on liquids, equivalent to about 3 K supercooling below T_{NAT}.

[17] Because of the importance of denitrification in this winter a parameterization for the sedimentation of NAT particles was introduced into the model [*Grooß et al.*, 2002]. Assuming that the aerosol is homogeneously distributed inside the air mass, the terminal settling velocity of the particles is computed to determine the mass flow out of the considered air parcel. In the model, this mass flow is controlled by an adjustable parameter, the so-called characteristic height. To determine the fraction of solid HNO_3 removed from the considered air mass, this parameter has to be adjusted to suitable NO_y measurements. NO_y measurements are, however, not available for all relevant altitudes and for all time periods of this study. Therefore we employed a characteristic height of 250 m that was deduced from comparisons with the ER-2 NO_y measurements [*Grooß et al.*, 2002] for a potential temperature of approximately 450 K and for the period of early February to mid-March. Although this reference height will not allow denitrification to be simulated accurately for all conditions considered, it is nonetheless suitable for exploring the sensitivity of our simulations to denitrification. In particular, during the chlorine activation period (approximately until late January/early February) the influence of denitrification on ClO_x, and thus the impact of the chosen characteristic height, is small (see section 4). Because this characteristic height is validated only for the March flight around 450 K, we will discuss our results compared to simulations without denitrification and will show that this parameterization is satisfactory for the purpose of this study. A sedimentation of ice particles leading to dehydration of the analyzed air parcels is not considered in the model simulations.

3.2. Model Study

[18] We conducted long-term simulations initialized for early winter to study the chlorine evolution during the winter and to answer the question of whether model

Table 1. Mixing Ratios of the Major Chemical Species Measured by MkIV on 3 December 1999 Used to Initialize the Model Simulations for the Flight on 27 January 2000[a]

Θ_{start}, K	380	409	437	463	486	514	534	577	610	684	722
Θ_{end}, K	350	375	400	425	450	475	490	525	550	600	620
N_2O, ppbv	287.86	259.02	215.88	172.87	129.17	71.26	51.00	26.27	13.02	6.69	7.20
Cl_y, ppbv	0.62	1.16	1.83	2.38	2.82	3.24	3.33	3.38	3.38	3.37	3.37
HCl, ppbv	0.52	0.86	1.22	1.45	1.72	2.04	2.16	2.40	2.52	2.48	2.48
$ClNO_3$, ppbv	0.09	0.28	0.49	0.66	0.79	0.89	0.89	0.78	0.70	0.72	0.72
ClO, pptv	0.0	0.0	110.6	241.2	286.1	286.3	257.6	183.2	149.5	153.6	152.8
HOCl, pptv	6.0	13.0	18.3	19.8	20.9	22.3	21.2	16.1	13.1	13.8	13.7
NO_y, ppbv	2.33	4.61	8.48	10.76	12.47	15.08	15.88	16.10	15.26	14.94	14.97
NO, ppbv	0.007	0.01	0.002	0.006	0.03	0.07	0.07	0.17	0.62	1.05	1.01
NO_2, ppbv	0.05	0.06	0.08	0.11	0.14	0.17	0.20	0.37	0.73	0.97	0.95
N_2O_5, ppbv	0.007	0.0	0.0	0.0	0.0	0.0	0.04	0.49	1.82	2.71	2.63
HNO_3, ppbv	2.15	4.25	7.91	9.97	11.50	13.93	14.62	13.75	9.55	6.76	7.01
HNO_4, pptv	10.2	6.4	0.0	0.2	2.0	5.7	8.0	13.3	17.6	15.1	15.5
O_3, ppmv	0.81	1.45	2.51	3.02	3.19	3.20	3.17	3.05	3.08	3.04	3.04
CH_4, ppmv	1.64	1.51	1.32	1.17	1.01	0.79	0.71	0.59	0.44	0.36	0.37
H_2O, ppmv	4.48	4.28	4.70	5.09	5.29	5.83	6.11	6.50	6.55	6.82	6.78

[a]The potential temperature values are shown for the trajectory start point on 3 December 1999 and for the trajectory end point on 27 January 2000.

simulations can reproduce the measured ClO mixing ratios and explain the quasi-simultaneously observed ozone loss. For these long-term simulations, backward trajectories were calculated from the locations of the measurement on 27 January 2000 and 1 March 2000 back to 3 December 1999 at different levels of potential temperature (Θ) between 350 and 620 K (Θ = 350 K, 375 K, 400 K, 425 K, 450 K, 475 K, 525 K, 550 K, 600 K, and in addition 620 K for January) for ascent and descent. At the maximum potential temperature only one backward trajectory is calculated for each flight. Backward trajectories starting at the float level (Θ = 490 K) were calculated for SZAs of 92°, 94°, 96°, and 98° for 27 January 2000 and for SZAs of 82°, 84°, 86°, and 88° for 1 March 2000. We calculated backward trajectories using wind data from the UK Met Office (UKMO) analysis taking diabatic descent into account [*McKenna et al.*, 2002a, 2002b]. Diabatic descent rates were calculated using a radiation model [*Zhong and Haigh*, 1995].

3.3. Initialization Procedure

[19] We initialized the simulations with prewinter reference data taken mostly from measurements of the OMS remote balloon flight launched on 3 December 1999 from Esrange (67.5°N, 21.0°E) near Kiruna. The OMS remote observations were obtained by the MkIV Solar Occultation Fourier Transform Infrared Spectrometer [*Toon et al.*, 1999]. To avoid possible inconsistencies of the initialization due to diabatic descent, we initialized the air parcels through correlations between mixing ratios of the specific chemical species and N_2O mixing ratios measured on the TRIPLE gondola by the cryogenic whole air sampler.

[20] Total inorganic chlorine (Cl_y) is determined from a Cl_y - N_2O correlation derived from measurements by the cryogenic whole air sampler on board TRIPLE on 27 January 2000 and on 1 March 2000 and measurements by the Airborne Chromatograph for Atmospheric Trace Species (ACATS) [*Elkins et al.*, 1996] on board the ER-2 aircraft during the SOLVE campaign [*Grooß et al.*, 2002, Table 1].

[21] The sum of chlorine species measured by MkIV (ClO, HOCl, $ClONO_2$, and HCl) was compared to Cl_y mixing ratios derived from Cl_y - N_2O correlation at the same N_2O levels. The derived difference was corrected by linearly scaling the chlorine species measured by MkIV, where the scaling factor ranges between 0.9 and 1.1.

[22] All other inorganic chlorine species are initialized as zero. Species of the nitrogen family, CH_4, H_2O, CO, H_2O_2, and O_3 were taken directly from the MkIV measurements based on N_2O without any scaling. Species of minor importance and not explicitly mentioned here were initialized using output from a simulation with the Mainz photochemical 2-D model [*Gidel et al.*, 1983; *Grooß*, 1996] because no measured data were available. Mixing ratios of the major chemical species used to initialize the model simulations are shown in Tables 1 and 2.

3.4. Sensitivity Studies

[23] The sensitivity of the model simulations toward the surface area of the background aerosol (SSA = stratospheric sulfuric aerosol) per unit volume A_{SSA} was examined. A_{SSA} was adjusted employing optical aerosol counter [*Deshler and Oltmans*, 1998] measurements from two flights of the HALOZ [*Vömel et al.*, 2001] and the PSC analysis [*Voigt et al.*, 2000; *Larsen et al.*, 2002; *Schreiner et al.*, 2002] payloads launched from Esrange on 19, 25, and 27 January 2000. We assume A_{SSA} does not change substantially up to 1 March 2000. For these tests the surface area of SSA particles per unit volume was adjusted by varying the mixing ratio of H_2SO_4 in ppbv in gas-phase equivalent (0.5, 0.05, and 0.01 ppbv H_2SO_4). Figure 3 shows the H_2SO_4 mixing ratios and the resulting A_{SSA} for both flights compared to the measurements.

[24] To determine the influence of denitrification by the sedimentation of large particles containing HNO_3, we performed long-term simulations with and without denitrification, as explained in section 3.1.

[25] In addition to model simulations using current recommendations for rate constants and absorption cross sections by *Sander et al.* [2000], further simulations with recently reported rate constants for the ClO self-reaction [*Bloss et al.*, 2001] were performed:

$$k_0(T) = (1.49 \pm 0.56) \times 10^{-32} \times (T/300)^{(-4.50 \pm 0.98)}.$$

The derived low pressure limit $k_0(T)$ of the termolecular reaction ClO + ClO + M $\rightarrow$ Cl_2O_2 + M is greater than

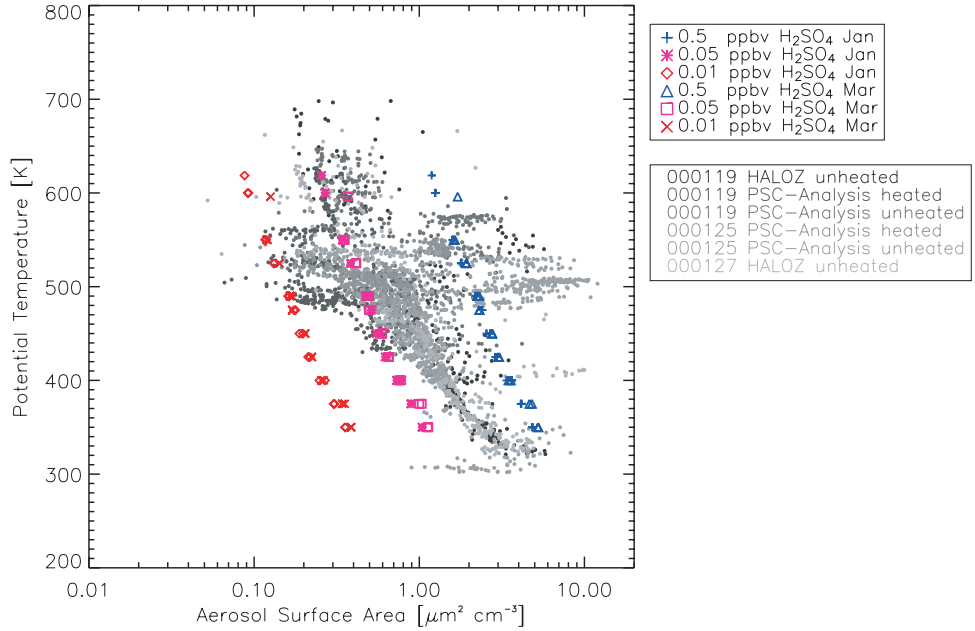

Figure 3. Simulated surface areas of SSA (stratospheric sulfuric aerosol) particle per unit volume A_{SSA} for the different levels of potential temperature for both flights in January and in March 2000 are compared to the measurement from 2 flights of both the HALOZ and the PSC analysis payloads (with heated or unheated inlet). In the microphysics module of CLaMS, A_{SSA} was adjusted by the input value of H_2SO_4 in gas-phase equivalent (see text).

recommended in the work of *Sander et al.* [2000]. We also performed simulations with maximum values of $k_0(T)$ adjusted to the upper limit of the error as derived by *Bloss et al.* [2001]:

$$k_0^{max}(T) = 2.05 \times 10^{-32} \times (T/300)^{-5.48}.$$

3.5. Studies on Uncertainties Along the Trajectories and on Uncertainties in Temperatures

[26] Our model simulations extend over a period of 2–3 months, although trajectories in the middle stratosphere can be considered to be quantitatively accurate for only up to ≈10 days [*Austin*, 1986]. Thus the photochemical history represented by a single trajectory of several months might differ from that experienced over the winter by the air sampled during the balloon flight. Therefore we performed studies to take into account the uncertainties arising from accumulated errors along the calculated backward trajectories. We calculated ensembles of 27 backward trajectories with the starting points grouped around the location of the measurements (±2° in latitude (≈ ±220 km) × ±5° in longitude (≈ ±390 km) × ±5 K in Θ) to obtain the dispersion of ClO in space, referred to in the following as clusters of trajectories.

[27] For levels of potential temperature greater than 400 K all trajectories for both flights remained inside the polar vortex during the simulated time period. Therefore considering the variation within one cluster of trajectories, we can assume that we studied typical vortex trajectories in winter 1999/2000. Between 350 and 400 K some trajectories originate from midlatitudes, so that uncertainties exist about the origin of the observed air parcels. At 350 K potential temperature approximately a third of the trajectories originate outside the polar vortex for both flights. At 375 K and 400 K only up to ≈3 individual trajectories within one cluster originate outside the vortex for 27 January 2000 whereas for 1 March 2000 all trajectories remained inside the vortex.

[28] Atmospheric mixing processes should be considered in simulating stratospheric chemistry. From our analysis, we obtained the information that the calculated backward trajectories within one cluster stayed close together during the winter (except at the lower levels). This is due to the fact that the Arctic winter 1999/2000 is characterized by a stable stratospheric circulation until mid-March [*Manney and Sabutis*, 2000]. *Konopka et al.* [2003] studied the impact of mixing processes on chlorine deactivation within the Arctic polar vortex 1999/2000. They found that the amount of $ClONO_2$ formed due to chemistry induced by mixing of the activated vortex air with NO_x-rich midlatitude air does not exceed 3% and the impact of mixing on the accumulated ozone loss is less than 1%. In our case, the trajectories remained inside the vortex (except at the lower levels) and the PV values along the trajectories show no evidence that air from midlatitude was mixed in. Thus we consider simulations presented here performed without mixing processes but considering uncertainties in the calculated air parcel position to be a good approximation.

[29] Further, we performed sensitivity calculations to test the impact of the reported uncertainties in temperatures derived from UKMO analyses [*Knudsen et al.*, 2001, 2002].

4. Results

4.1. ClO Model Results

[30] The dynamic and chemical evolution along the model trajectories depends on altitude. To discuss the model results in comparison with the measurements we classify the

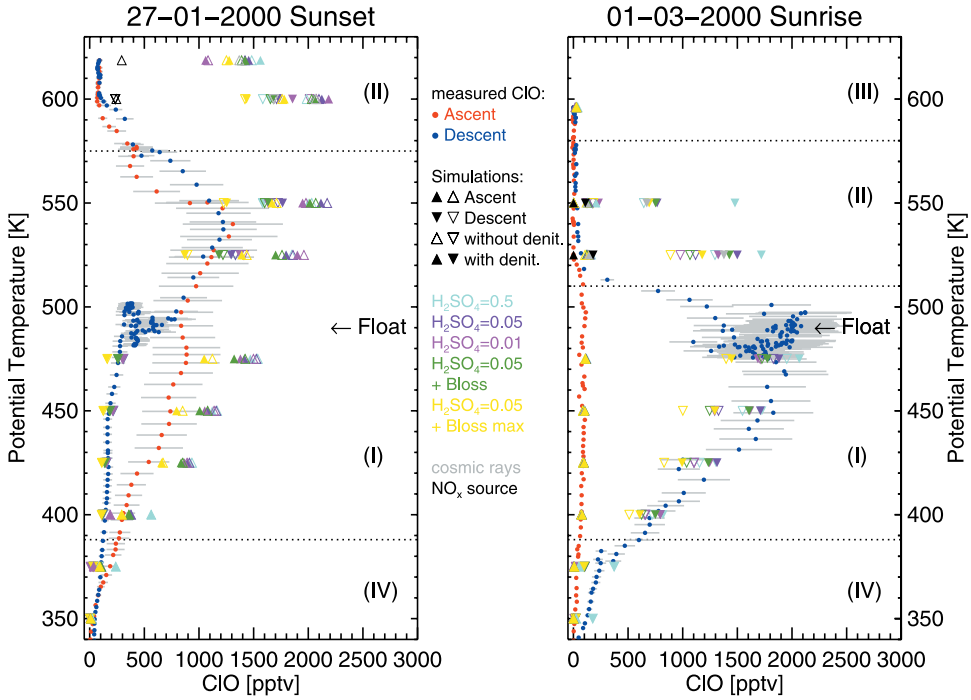

Figure 4. Measured ClO mixing ratios (blue and red dots, as in Figure 2) in comparison to different simulated ClO mixing ratios for (left) 27 January 2000 and for (right) 1 March 2000. The simulated ClO mixing ratios for ascent are marked by black and white upward triangles and for descent by black and white downward triangles. Sensitivity tests with respect to the surface area of the background aerosol per unit volume A_{SSA} (adjusted by prescribing H_2SO_4 in ppbv in the gas phase, see text) and to different kinetics of ClO self-reaction (see text) are marked by different colors (see legend). Simulated ClO mixing ratios derived by simulations without denitrification (white upward and downward triangles) are compared to simulated ClO mixing ratios derived by simulations with denitrification (black upward and downward triangles; see text). Simulated ClO mixing ratios are classified according to different characteristics (see text), which are marked by (I) activated layer, (II) NO_x-determined layer, (III) the top altitude on March and (IV) the lowest layer. The float altitude at Θ = 490 K is marked by an arrow. For the NO_x-determined layer (II) long-term simulations considering the effect of cosmic rays (gray) and an effective NO_x source (black) are also shown (see text).

simulated ClO mixing ratios according to the different characteristics obtained for the two flights.

4.1.1. Activated Layer (I)

[31] Simulations along model trajectories ending between 400 and 550 K potential temperature on 27 January 2000 and between 400 and 490 K potential temperature on 1 March 2000 are characterized by PSC occurrence during the winter due to low temperatures. Simulated ClO mixing ratios indicate full chlorine activation due to heterogeneous chemistry on PSCs. In the following we refer to this region of potential temperature as the activated layer.

[32] For both flights, NAT and liquid ternary solution particles were formed for all model trajectories located in the activated layer. The formation of ice particles is confined to only a few trajectories in a short time period due to the temperature evolution during the winter.

[33] Figure 4 shows simulated ClO mixing ratios as a function of potential temperature from model calculations for different assumptions on the surface area of the background aerosol per unit volume A_{SSA}, on denitrification, and on the kinetics of ClO self-reaction in comparison with the ClO measurements for both TRIPLE flights. The activated layer is denoted by (I). In Figure 5 the same simulated ClO mixing ratios are shown in comparison to the measurements as a function of solar zenith angle (SZA).

[34] On 27 January simulated ClO mixing ratios for different assumptions on A_{SSA} and on denitrification agree within the uncertainties of the ClO measurement for float and night conditions (see Figures 4 and 5). All simulations for daylight conditions encountered during ascent are ≈30% greater than the ClO measurements, except for Θ = 400 K. Here only simulations with H_2SO_4 = 0.5 ppbv overestimate the ClO measurements (see Figure 4). Our studies show similar as the model study by *Drdla and Schoeberl* [2002] that during the chlorine activation period the impact of denitrification on ClO_x mixing ratios is small. Therefore the simulated ClO mixing ratios show only a weak sensitivity to the assumed extent of denitrification. When using the rate coefficient of the ClO self-reaction reported by *Bloss et al.* [2001], the simulations also overestimate the measured ClO mixing ratios during daylight, but agree very well with the ClO measurements in darkness and twilight during descent and float. In contrast, when using the upper limit for this reaction $k_0^{max}(T)$ the simulated ClO mixing ratios agree with the ClO measurements for daylight, but underestimate

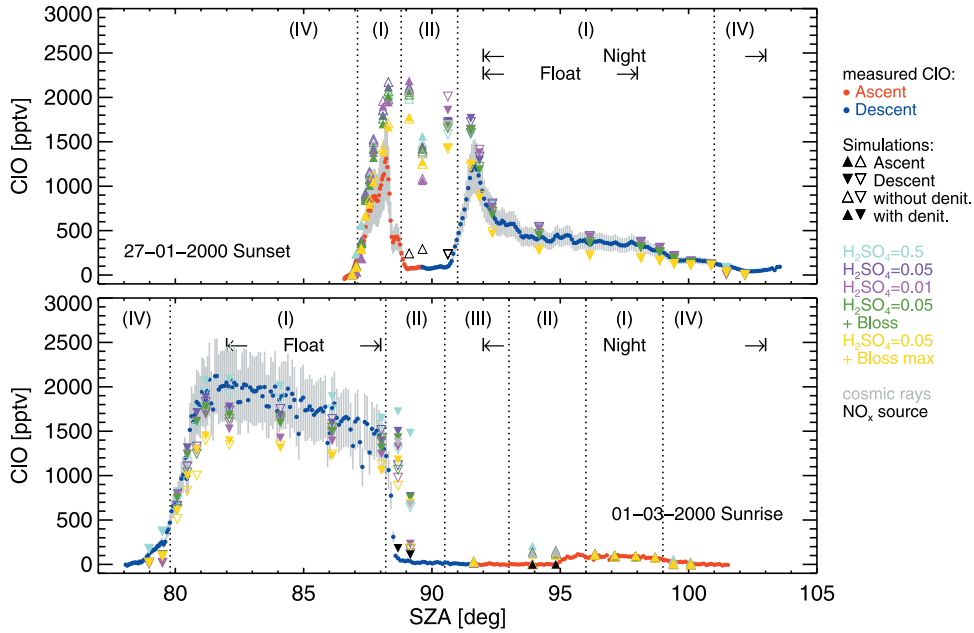

Figure 5. Same measured ClO mixing ratios compared to same simulated ClO mixing ratios as in Figure 4, but as a function of solar zenith angle (SZA) for (top) 27 January 2000 and for (bottom) 1 March 2000. Both the float level at 490 K potential temperature and the nighttime are marked by arrows. Further, the activated layer (I), the NO_x-determined layer (II), the top altitude on March (III), and the lowest layer (IV) are also marked.

somewhat the measured ClO mixing ratios in descent and float.

[35] On 1 March for the activated layer, simulated ClO mixing ratios show a good overall agreement with the measurements, but some simulated ClO mixing ratios are at the low end of the error bars (see Figures 4 and 5). The sensitivity with respect to A_{SSA} and to denitrification is within approximately 25%. Simulated ClO mixing ratios performed with rate constants reported by *Sander et al.* [2000] and by *Bloss et al.* [2001] agree very well with measured ClO mixing ratios for both daylight and night, while ClO mixing ratios simulated with $k_0^{max}(T)$ values underestimate the measured ClO mixing ratios by a maximum value of ≈30% at 450 K potential temperature. In contrast to the January flight, the characteristic height of 250 m optimized for the February–March period (see section 3.1) is a satisfactory parameterization. Thus overall for 1 March the best agreement between simulated and measured ClO mixing ratios seems to be obtained for simulations with denitrification.

4.1.2. NO_x-Determined Layer (II)

[36] Simulations along model trajectories ending at 600 K and 620 K potential temperature on 27 January 2000 and ending at 525 K and 550 K potential temperature on 1 March 2000 are also characterized by PSC occurrence during the winter due to low temperatures. Observations obtained by the POAM III (Polar Ozone and Aerosol Measurement) satellite instrument also show that PSCs occurred at these levels of potential temperature during the Arctic winter 1999/2000 [*Bevilacqua et al.*, 2002]. For all the simulations performed, measured ClO mixing ratios of approximately 100 pptv were overestimated by approximately a factor of 10–20 (see Figure 4). In the Arctic, chlorine deactivation proceeds via the formation of $ClONO_2$ [*Douglass et al.*, 1995], thus the rate of deactivation is determined by the available NO_x. Therefore we termed this layer, where chlorine deactivation proceeds in January and is completed in March, the NO_x-determined layer denoted by (II). The following different mechanisms producing additional NO_x in the gas phase were studied:

[37] 1. A possible NO_x source is the suppression of the heterogeneous hydrolysis of N_2O_5 ($N_2O_5 + H_2O \rightarrow 2HNO_3$), thus removing a NO_x sink. To test this we reduce aerosol surfaces areas. However, even for A_{SSA} of about 0.005–0.008 [μm^2 cm^{-3}] (equivalent to H_2SO_4 = 0.005 ppbv), which is a factor of 10 below the minimum measured on the HALOZ payload, the simulated ClO mixing ratios are still substantially greater than the measured ClO mixing ratios. We also analyzed the sensitivity to the reaction probability γ within the uncertainties [*DeMore et al.*, 1997], but also here the simulated ClO mixing ratios are substantially greater than the measured ClO mixing ratios. Only for γ close to zero can simulations reproduce the observed ClO mixing ratios.

[38] 2. We performed model simulations using two different schemes of heterogeneous chemistry parameterizations first by *Abbatt and Molina* [1992] and *Zhang et al.* [1994] and second by *Hanson and Ravishankara* [1993]. These differ in the heterogeneous reactions rates of $ClONO_2$ with HCl and H_2O on NAT and SAT particles. *Carslaw et al.* [1997] found substantial differences between the two schemes in chlorine activation in early winter. However, we found no significant difference between the simulated ClO mixing ratios for these two parameterizations. Nor can the different schemes of heterogeneous chemistry parameterizations explain the low ClO mixing ratios measured.

Table 2. Mixing Ratios of the Major Chemical Species Measured by MkIV on 3 December 1999 Used to Initialize the Model Simulations for the Flight on 1 March 2000[a]

Θ_{start}, K	394	420	450	468	490	525	550	612	667	838
Θ_{end}, K	350	375	400	425	450	475	490	525	550	600
N_2O, ppbv	282.09	259.33	205.27	155.06	93.30	37.52	26.07	6.22	3.33	1.14
Cl_y, ppbv	0.73	1.15	1.98	2.57	3.11	3.36	3.38	3.37	3.37	3.36
HCl, ppbv	0.59	0.86	1.25	1.57	1.92	2.26	2.40	2.47	2.37	2.24
$ClNO_3$, ppbv	0.14	0.28	0.47	0.72	0.86	0.86	0.78	0.73	0.78	0.83
ClO, pptv	0.0	0.0	170.1	262.3	301.9	225.5	182.4	157.5	207.0	279.1
HOCl, pptv	7.7	12.9	18.7	20.2	22.3	19.4	16.0	13.7	12.6	14.6
NO_y, ppbv	2.89	4.60	9.36	11.44	14.03	16.21	16.09	14.89	13.93	11.47
NO, ppbv	0.01	0.01	0.007	0.01	0.06	0.09	0.18	1.12	2.11	3.33
NO_2, ppbv	0.05	0.05	0.09	0.13	0.16	0.24	0.37	0.99	1.41	1.95
N_2O_5, ppbv	0.004	0.0	0.0	0.0	0.0	0.14	0.50	2.75	2.48	1.35
HNO_3, ppbv	2.68	4.23	8.73	10.57	12.93	14.74	13.73	6.93	4.66	2.66
HNO_4, pptv	9.2	6.4	0.8	0.9	3.8	8.4	13.4	15.4	8.9	3.8
O_3, ppmv	0.96	1.45	2.72	3.10	3.21	3.13	3.05	3.05	3.18	3.04
CH_4, ppmv	1.61	1.51	1.28	1.11	0.87	0.65	0.58	0.36	0.29	0.17
H_2O, ppmv	4.36	4.28	4.83	5.16	5.55	6.34	6.50	6.85	6.94	6.96

[a]The potential temperature values are shown for the trajectory start point on 3 December 1999 and for the trajectory end point on 1 March 2000.

[39] 3. We studied the impact of galactic cosmic rays at these altitudes. We implemented a NO_x source due to ionization processes of galactic cosmic rays in the CLaMS model using a parameterization derived by *Heaps* [1978]. The ionization rate caused by galactic cosmic rays depends on magnetic latitude Λ, on total number density of air molecules N, and on altitude [e.g., *Neher*, 1961, 1967, 1971]. We used two parameterizations to compute the ion-pair production of solar minimum (equivalent to galactic cosmic ray maximum) for Λ equatorward and poleward of 60 degrees and assumed a production of 1.5 NO molecules per ionized molecule (N_2 and O_2) [*Crutzen et al.*, 1975]. From this, we computed a NO production rate of approximately 10–40 [molecules cm^{-3} s^{-1}]. Figures 4 and 5 show that simulated ClO mixing ratios considering galactic cosmic rays still overestimate measured ClO mixing ratios.

[40] 4. We deduced the magnitude of a potential NO_x source that would be necessary to roughly reproduce the measured ClO mixing ratios ($\approx$100 pptv) in the model. We employ the same parameterization as for the cosmic ray case, but introduce a simple multiplication factor (see Figures 4 and 5). From the simulations it is inferred that a permanent NO_x emission rate of 300–1000 [molecules cm^{-3} s^{-1}] is required. Such a NO_x emission rate yields simulated mixing ratios of up to 2 ppbv NO_x for 27 January 2000 and up to 0.7 ppbv NO_x for 1 March 2000. The simulations for 27 January 2000 were performed without denitrification and for 1 March 2000 with denitrification. It is also necessary to assume denitrification in simulations for 1 March 2000 in order to reproduce the HCl and NO_x mixing ratios measured by HALOE (see below in section 4.3).

[41] Transport of NO_x-rich air from the mesosphere and the upper stratosphere to the lower stratosphere could be a potential NO_x source [e.g., *Callis and Lambeth*, 1998; *Jackman et al.*, 2000; *Callis et al.*, 2001]; unfortunately we have no means of checking the likelihood of this assumption.

4.1.3. Top Altitude on 1 March (III)

[42] On 1 March 2000 the ClO measurement at about 600 K potential temperature yielded low ClO mixing ratios $\ll$ 100 pptv. ClO mixing ratios obtained from long-term simulations agree well with the observations (see Figure 4, denoted by (III)). PSCs were not computed in the model simulations ending at 600 K potential temperature, so that no chlorine activation occurred along the model trajectories in contrast to the model simulations ending at 550 K. Thus the upper limit to the PSC occurrence altitude can be inferred from these results to be between 550 K and 600 K potential temperature. The minimum temperatures of the model trajectories at Θ = 600 K are around 192 K in comparison to 184 K minimum temperature for the Θ = 550 K trajectory (according to UKMO analysis). The air masses at Θ = 600 K originate from very high levels of potential temperature in December ($\Theta \approx$850 K) (see Table 2). The simulated PSC existence altitudes are consistent with a model analysis for the Arctic winter 1999/2000 by *Rex et al.* [2002] based on PSC observations by the POAM III satellite instrument and by ground-based lidar observations.

4.1.4. Lowest Layer (IV)

[43] The model trajectories at 350 and 375 K potential temperature are characterized by a small amount of chlorine activation on the surface of SSA particles, labeled (IV) in Figure 4. The minimum temperatures of the model trajectories are above the formation temperatures of ternary solution and NAT particles so that only SSA particles exist. Figure 4 shows that simulated ClO mixing ratios are sensitive to the assumed surface area of SSA particles. Best agreement between simulated and measured ClO mixing ratios is obtained for a surface area of SSA particles per unit volume between 4.0 and 5.0 [μm^2 cm^{-3}] (equivalent to 0.5 ppbv H_2SO_4 in the gas phase). For 350 K potential temperature, the simulated surface areas of SSA particles are at the upper limit of the particle measurements on board the HALOZ and the PSC analysis payload. For 375 K potential temperature, the simulated ClO mixing ratios with 0.5 ppbv H_2SO_4 in the gas phase are somewhat higher than the measured ClO mixing ratios because the surface area of SSA particles employed in model simulations is also somewhat higher than the measured surface area of SSA particles. For lower A_{SSA} values, the simulations cannot reproduce the measured ClO mixing ratios of up to about 300 pptv. Simulations show that on 27 January a small fraction of the available amount of the reservoir species HCl

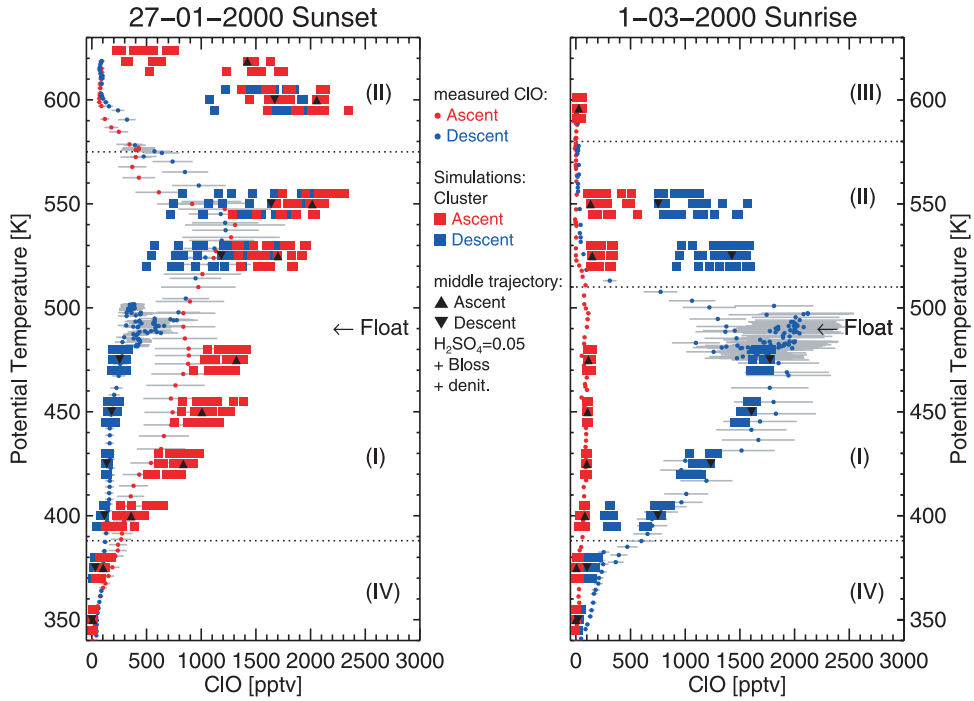

Figure 6. Measured ClO mixing ratios (blue and red dots, as in Figure 2) compared to simulated ClO mixing ratios derived within the framework of dynamic sensitivity tests. Simulated ClO mixing ratios are shown for clusters of backward trajectories (red squares for ascent, blue squares for descent) with the starting points grouped around the location of the measurements (±2° in latitude, ±5° in longitude and ±5 K in Θ). For this dynamic sensitivity test simulations were performed with denitrification, A_{SSA} values corresponding to H_2SO_4 = 0.05 ppbv in gas-phase equivalent and kinetics of ClO self-reaction $k_0(T)$ by *Bloss et al.* [2001], which yielded the best overall agreement with ClO measurements of both flights and are denoted as standard. The simulated ClO mixing ratios for the central trajectory within one cluster are denoted by black triangles. The same terminology for the classified areas is used as in Figure 4.

had reacted on the surface of the SSA particles to form active chlorine and that by 1 March nearly the total available amount of HCl had been activated (see Figure 8 below).

4.2. Results of Studies on Uncertainties Along the Trajectories and on Uncertainties in Temperatures

[44] Sensitivity studies on uncertainties arising from accumulated errors along the calculated backward trajectories were performed. We calculated clusters of backward trajectories with the starting points grouped around the location of the measurements (see section 3.2) to examine the variability of the chlorine chemistry due to dynamic variations.

[45] We chose the model simulation with denitrification, A_{SSA} values corresponding to H_2SO_4 = 0.05 ppbv in gas-phase equivalent and kinetics of ClO self-reaction $k_0(T)$ by *Bloss et al.* [2001], which yielded the best overall agreement with ClO measurements for both flights as the standard. Figure 6 shows the model results for the clusters of backward trajectories compared to the ClO measurements. The variation in the simulated ClO mixing ratios within a cluster of trajectories is a measure of the uncertainty in the simulated values due to uncertainties in the air parcel history.

[46] In the activated layer (I) all trajectories remain inside the polar vortex and experience similar temperature and PSC conditions. The variation of simulated ClO mixing ratios within a cluster on 27 January 2000 for 400–475 K is ≈500 pptv for daylight conditions and for 525 K and 550 K is somewhat greater, ≈700 pptv, because of the high variability of SZA at the endpoints of the individual trajectories within the cluster. The variation of simulated ClO mixing ratios within a cluster on 1 March 2000 is smaller ≈300 pptv for daylight conditions, except for some trajectories at 400 K, where temperatures are warmer so that no PSCs occur on some trajectories. Simulated ClO mixing ratios for such trajectories are obviously lower than the measured ClO mixing ratios.

[47] In the NO_x-determined layer (II) all trajectories remain inside the vortex, but on 27 January 2000 some trajectories at 620 K do not experience PSC conditions because the temperatures are too warm and thus no chlorine activation was simulated. The variation of simulated ClO mixing ratios within a cluster is ≈1000 pptv for daylight conditions (except on 27 January 2000 at 620 K). Nevertheless, uncertainties arising from accumulated errors along the model trajectories cannot explain the low measured ClO mixing ratios (≈100 pptv).

[48] In the lowest layer between 350 and 375 K (IV) some trajectories originate from midlatitudes. The observed air masses most likely contain a mixture of midlatitude and vortex air. Thus the variation of simulated ClO mixing ratios within one cluster of trajectories represents the

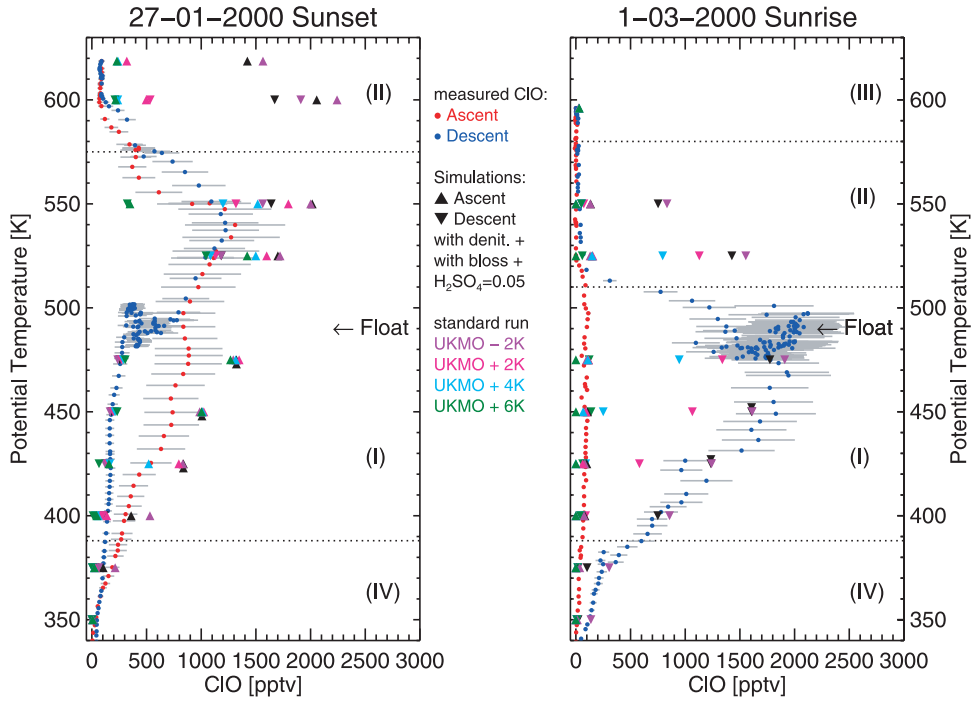

Figure 7. Measured ClO mixing ratios (blue and red dots, as in Figure 2) compared to simulated ClO mixing ratios derived by sensitivity test due to temperature effects. The temperatures along the trajectories were modified by the addition and subtraction of fixed temperature intervals of −2 K, +2 K, +4 K, and +6 K (see legend). These simulations are also performed under standard conditions as explained in Figure 6. Some symbols denoting the standard model simulation are vertically shifted to distinguish between the different model simulations.

uncertainties in the air parcel origin. For both flights, simulated daylight ClO mixing ratios at 350 K potential temperature amount to approximately 100 pptv and at 375 K potential temperature range approximately between 100 and 200 pptv.

[49] Sensitivity studies were performed (Figure 7) to investigate the influence on the simulated chlorine activation of uncertainties in UKMO temperatures of up to ±5 K reported by *Knudsen et al.* [2002] for the Arctic winter 1999/2000. The temperatures along the trajectories were modified by a constant offset of −2 K, +2 K, +4 K, and +6 K. Here we mainly used higher temperatures since for the January flight ClO measurements were less than ClO simulations, thus suggesting less chlorine activation in reality than in the model.

[50] The time evolution of ClO_x along the different trajectories is very different due to their individual temperatures. However, for the January flight the apparent sensitivity of temperature effects for the trajectories at 450 K and 475 K potential temperature within the activated layer is quite small (see Figure 7). The reason is that the temperature minimum occurs in early January and therefore NAT formation occurs along these trajectories. Thus irrespective of the chosen temperature offset sufficient NAT activity occurs in mid-January so that shortly afterward, on 27 January 2000 no substantial impact of the temperature offset is noticeable. In mid-January, $ClONO_2$ is completely activated, and HCl mixing ratios have been reduced to approximately the same amount along each of these trajectories causing approximately the same ClO_x mixing ratios. In contrast, for the March flight, the influence of temperature changes is evident due to the different PSC occurrence along the individual trajectories and resultant chlorine activation meaning that for warmer temperatures the simulated ClO mixing ratios are much lower than the measured ClO mixing ratios.

[51] Within the NO_x-determined layer the simulated ClO mixing ratios agree with the measured ClO mixing ratios for temperatures of 4–6 K higher than the temperatures obtained from UKMO for the January flight and for temperatures of 2–6 K higher than the temperatures obtained from UKMO for the March flight. In simulations with those trajectories, the chlorine activation was suppressed due to the absence of PSCs. However, such a low bias in the UKMO temperatures could not be a viable explanation for the high ClO mixing ratios simulated for the March flight (see section 5).

[52] Within the lowest layer, simulations along trajectories modified by a constant offset of −2 K yielded the best agreement with the measurements.

4.3. Comparison of Simulated HCl and NO_x Mixing Ratios With HALOE Observations

[53] To corroborate the results of the model simulations we compare the simulated HCl and NO_x (NO_x = NO + NO_2) mixing ratios for 1 March 2000 with measurements by the HALOE instrument on board the UARS satellite [*Russell et al.*, 1993]. Figure 8 shows HALOE measurements obtained inside the vortex [*Müller et al.*, 2002] for the time period between 19 and 26 February 2000 compared to results of simulations for 1 March 2000.

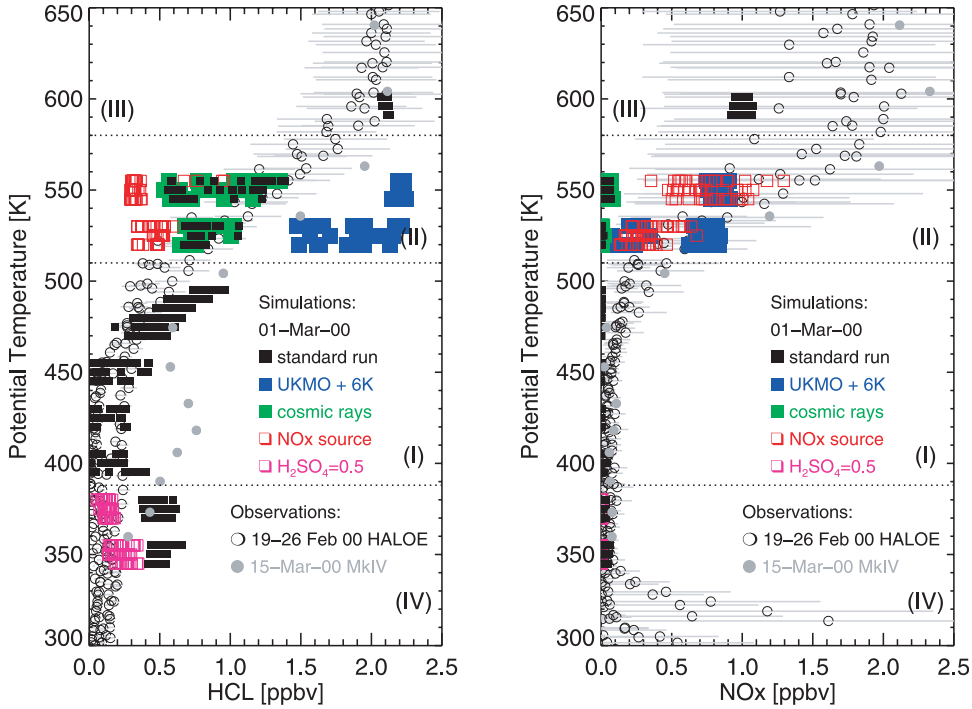

Figure 8. (left) Measured HCl mixing ratios and (right) NO_x(= NO + NO_2) mixing ratios obtained by HALOE (circles) inside the Arctic polar vortex between 19 and 26 February 2000 (PV $\geq$ 50 PVU at 475 K, PV $\geq$ 100 PVU at 550 K, and PV $\geq$ 200 PVU at 675 K; same profiles as chosen in the work of *Müller et al.* [2002]) are compared to simulated HCl and NO_x mixing ratios for 1 March 2000. The HALOE data processing version 19 is used. The accuracy of the HCl measurement (gray bars) is 14–24% between 10 and 100 hPa [see *Müller et al.*, 2002, Table 2]. The accuracy of the NO and NO_2 measurements (gray bars) is 102% and 100% between cloud height and 25 km altitude [*Gordley et al.*, 1996]. Simulated HCl and NO_x mixing ratios are shown for clusters of trajectories under standard conditions (black squares), same simulation as shown for ClO mixing ratios in Figure 6, but in addition simulations for the float level at 490 K are also shown. Further, for the NO_x-determined layer (II) and the lowest layer (IV) simulated HCl and NO_x mixing ratios derived by sensitivity tests are plotted (see legend and text). In addition HCl and NO_x mixing ratios measured by MkIV on 15 March 2000 on board OMS payload also launched from Kiruna are shown (gray dots).

[54] HCl is a measure of the temporal evolution of the chlorine activation and deactivation throughout the winter. At the end of February small HCl mixing ratios of $\leq$ 0.5 ppbv are observed between 350 and 500 K indicating almost complete chlorine activation. The HCl observations of about 2.0 ppbv at 600 K potential temperature are equivalent to the prewinter reference values (see Table 2) indicating no chlorine activation. Between 525 and 550 K, measured HCl mixing ratios increase from 0.5 ppbv to 1.7 ppbv.

[55] The observed NO_x mixing ratios are consistent with the previously derived mechanisms. In the activated layer (I) between 400 and 500 K, NO_x mixing ratios are lower than 0.3 ppbv and thus unable to deactivate chlorine. Above 500 K, the observed NO_x mixing ratios increase to about 2.0 ppbv so that sufficient NO_x is available to deactivate chlorine.

[56] In Figure 8 the results for the standard model simulation with denitrification, A_{SSA} values corresponding to H_2SO_4 = 0.05 ppbv in gas-phase equivalent and kinetics of ClO self-reaction $k_0(T)$ by *Bloss et al.* [2001] are shown for all altitudes. Simulated NO_x mixing ratios agree with the HALOE observations in the lowest layer (IV) and the activated layer (I), except for 475 K and 490 K potential temperature, where the simulated NO_x mixing ratios are at the lower limit of the uncertainties of the measurements. At the top altitude (III) on 1 March 2000, simulated NO_x mixing ratios agree with the observations taking into account the uncertainties of the HALOE measurements. Simulated HCl mixing ratios also agree with the HCl mixing ratios measured by HALOE in the activated layer (I) and at the top altitude (III).

[57] In the lower layer, HCl mixing ratios simulated under standard conditions overestimate the HCl measurements because simulated chlorine activation is too weak (see Figure 4). In Figure 8 (pink squares) simulated HCl and NO_x mixing ratios are also shown which were computed with A_{SSA} values corresponding to H_2SO_4 = 0.5 ppbv in the gas-phase equivalent (here the JPL kinetic values are used). In this region higher SSA values than in the standard configuration are necessary to reproduce best ClO as well as HCl and NO_x mixing ratios by model simulations. This is consistent with the PSC measurements by the HALOZ and PSC analysis payloads as Figure 3 shows. In this region differences in the ClO self-reaction kinetics are of minor significance (see, e.g., Figure 4).

[58] For the NO_x-determined layer, in Figure 8 the simulated HCl and NO_x mixing ratios are additionally shown for some sensitivity studies. In fact, the standard simulation reproduces measured HCl mixing ratios, but not measured NO_x and ClO mixing ratios. Simulations assuming errors in UKMO temperatures of +6 K (resulting in no chlorine activation during the winter) can reproduce measured ClO and NO_x mixing ratios, but not measured HCl mixing ratios. Simulations assuming the influence of galactic cosmic rays fail to reproduce measured ClO and NO_x mixing ratios. In the NO_x-determined layer, several simulated HCl and NO_x mixing ratios, assuming a hypothetical NO_x source that reproduces roughly measured ClO mixing ratios, agree with HALOE measurements taking into account their uncertainties for both HCl and NO_x. However, at 550 K several simulated HCl mixing ratios underestimate the measured HCl values by up to a factor of 2. Nevertheless, simulations assuming an additional NO_x source can best simultaneously explain the measurements of the species ClO, HCl, and the total amount of NO and NO_2 (=NO_x).

[59] To deactivate chlorine there are in principle two reaction channels, first the reaction of ClO with NO_2 forming $ClONO_2$ and, second, the reaction of Cl with CH_4 forming HCl. To simulate HCl mixing ratios of 0.5–1.5 ppbv in the NO_x-determined layer, we must assume that denitrification occurred. In Figure 9 simulation results with denitrification are compared to those without denitrification as a function of time. For both simulations an additional NO_x source was assumed. Simulations performed without denitrification produce widespread occurrence of NAT particles in February 2000 in contrast to the simulations performed with denitrification. Thus for model simulations without denitrification, chlorine is reactivated via heterogeneous reactions so that HCl mixing ratios decline. The additional NO_x source is necessary to deactivate chlorine rapidly enough via the $ClONO_2$ channel. Thus to reproduce measured ClO and HCl mixing ratios by model simulations we must assume denitrification. NO_x mixing ratios, simulated for end of February assuming denitrification, are somewhat lower than the HALOE measurements due to the strong denitrification assumed in this model study.

[60] In Figure 8, we additionally show HCl and NO_x mixing ratios measured by MkIV on 15 March 2000 on board the OMS payload also launched from Esrange, Kiruna. This measurement was performed 2 weeks after the TRIPLE measurement and illustrates that chlorine deactivation continued inside the Arctic vortex 1999/2000. At all altitudes HCl mixing ratios increase between mid-February and mid-March indicating that deactivation proceeds, except at the top level (III) where no activation had taken place. In the lowest layer (IV) and in the activated layer (I), no significant change in NO_x mixing ratios is found. In the NO_x-determined layer (II) and at the top altitude (III) a small increase in NO_x mixing ratios is noticeable.

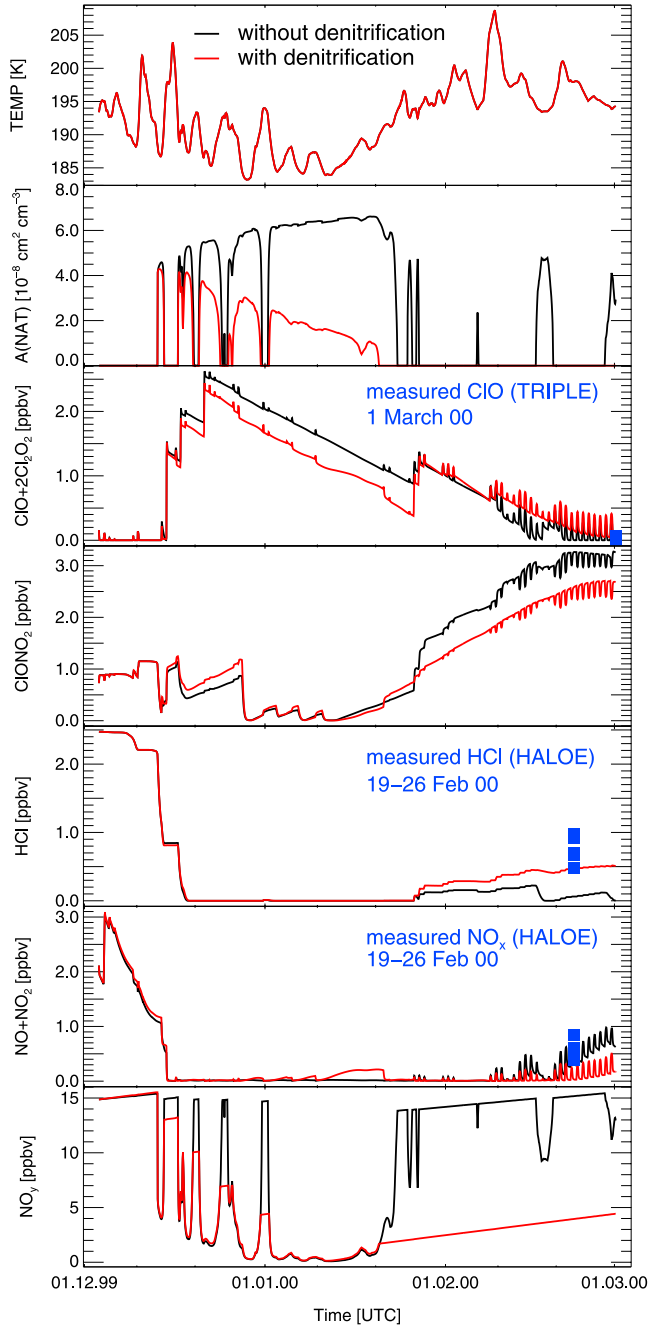

Figure 9. Simulated time-dependent behavior of key chemical species for the NO_x-determined layer (II) at 525 K are shown for 1 March 2000. Model simulations with (red lines) and without (black lines) denitrification are compared. For both simulations an additional NO_x source (see text) was assumed. Measured ClO (by TRIPLE), HCl, and NO_x (by HALOE) mixing ratios are also shown (blue squares).

4.4. Simulated Ozone Loss in Comparison to Observations

[61] Chemical ozone loss in the polar vortex can be estimated from changes in the relation between the mixing ratios of O_3 and a long-lived tracer like CH_4 assuming that the O_3 - tracer relation is not substantially affected by mixing processes [e.g., *Müller et al.*, 2002]. Owing to the stable polar vortex in winter 2000, the impact of mixing processes on the O_3 tracer relation over the period in question may be neglected [*Ray et al.*, 2002; *Salawitch et al.*, 2002].

[62] Figure 10 (bottom panel) shows the CH_4 - O_3 correlation for 3 December 1999 observed by MkIV as well as for 27 January 2000 and 1 March 2000 observed by

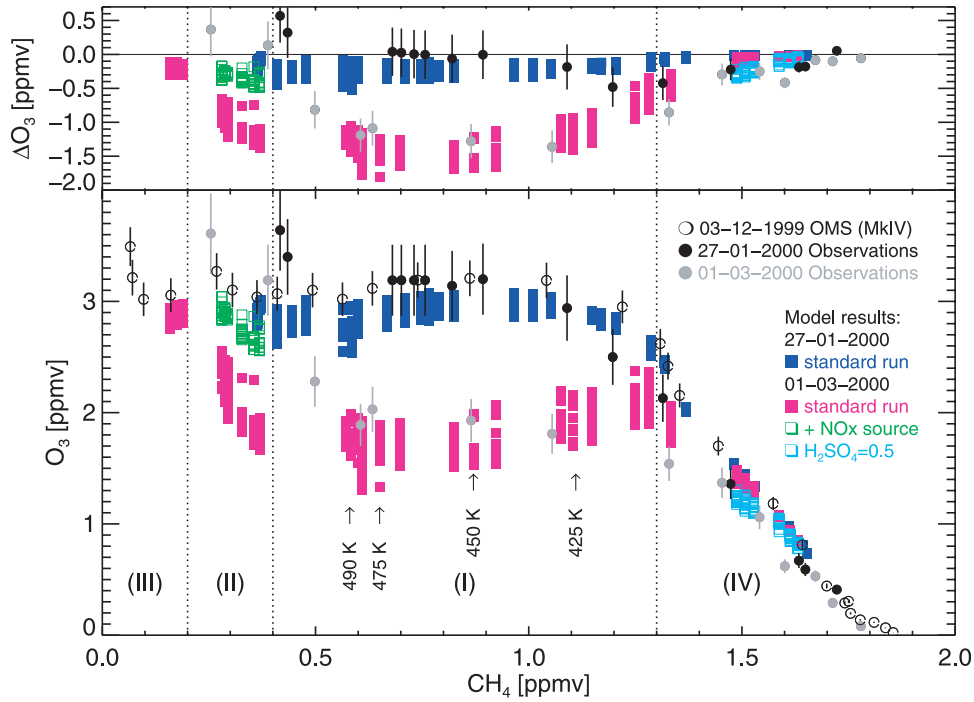

Figure 10. (top) Observed ozone loss as a function of CH_4 between 3 December 1999 and 27 January 2000 (black dots) and 1 March 2000 (gray dots), respectively, are shown in comparison to simulated ozone loss (blue squares for 27 January 2000 and pink squares for 1 March 2000). Simulations are performed for clusters of trajectories under standard conditions (see Figures 6 and 8). Further, for the NO_x-determined layer (II) and the lowest layer (IV) simulated ozone losses derived by sensitivity tests are plotted (see legend and text). Up to 27 January 2000 no significant ozone loss is derived. Up to 1 March 2000 a simulated ozone loss of about 0.8–1.8 ppmv was deduced between 425 and 490 K, with a maximum ozone loss of 1.8 ppmv at Θ = 475 K. (bottom) Measured O_3-CH_4 correlations from 27 January 2000 (black dots) and 1 March 2000 (gray dots) are shown in comparison to simulated O_3-CH_4 correlations (see top panel). In addition, the observed prewinter reference O_3-CH_4 correlation (circles) obtained by MkIV (OMS) on 3 December 1999 and used to initialize the simulations is shown. In the earlier figures (e.g., Figure 4), the simulated ClO mixing ratios are classified according to different characteristics. Here we used the same terminology on equivalent CH_4 levels. In the activated layer the corresponding levels of potential temperature for the March flight are labeled with arrows.

TRIPLE. The accuracy of MkIV measurements of CH_4 and O_3 is ≈5%. The analytical precision of the gas-chromatography measurements of CH_4 [*Levin et al.*, 1999] of the air samples collected by the cryogenic whole air sampler in the TRIPLE flights is 3 ppb (0.2–0.6%) and the accuracy of a well-prepared ozonesonde is 5–10% [*Harris et al.*, 1998]. Further, the observed ozone losses as a function of CH_4 between 3 December 1999 and both 27 January 2000 and 1 March 2000 are shown in Figure 10 (top panel). We calculate an overall uncertainty for the observed ozone losses by combining the individual terms of the ozone measurements in a "root of sum of squares" fashion. Between 3 December 1999 and 27 January 2000 the derived ozone loss is 0.5 ± 0.3 ppmv at about 425 K potential temperature (≡ 1.2–1.3 ppmv CH_4) and much lower elsewhere. By 1 March 2000 a significant ozone loss of about 0.8–1.4 ppmv is evident between 400 and 500 K potential temperature (≡ 0.5–1.3 ppmv CH_4) with a maximum value of 1.4 ± 0.2 ppmv at around 425 K.

[63] At high altitudes (CH_4 mixing ratio <0.5 ppmv corresponding to Θ > 600 K for 27 January 2000 and Θ > 500 K for 1 March 2000) measured ozone loss has a positive sign because ozone mixing ratios measured by MkIV on 3 December 1999 are lower than those of 27 January 2000 and of 1 March 2000. Reasons for this could be that at these altitudes the data quality of the ozonesonde (ECC) measurements decreases and the atmospheric variability of O_3 in the vortex in November/December was high [*Müller et al.*, 2002; *Salawitch et al.*, 2002].

[64] Figure 10 also shows simulated ozone loss and simulated ozone mixing ratios as a function of simulated CH_4 mixing ratios for clusters of trajectories under standard simulation conditions (see section 4.2). For 27 January 2000, model simulations show no substantial ozone depletion (averaging 0.2–0.3 ppmv). The observed small amount of ozone loss at around 425 K potential temperature (of up to −0.5 ppmv) is not reproduced by model simulations. The ozone-tracer correlation method is designed to quantify ozone loss accumulated over the winter and is thus not well suited to detect such small discrepancies. Indeed the ozonesonde measurements on 27 January 2000 at ≈425 K would be consistent with the simulations taking into account their uncertainties, so that no firm conclusions about the origin of the noted discrepancies between simulations and

measurements are possible. Except for these altitudes and the positive ΔO_3 values diagnosed for potential temperatures above 600 K the simulated ozone losses overestimate the observed ozone losses by a small amount of approximately 0.1 ppmv. The simulated ozone loss for 27 January 2000 must be considered as an upper limit because for these conditions the simulated ClO mixing ratios lie at the upper limit of the error bars of the observations.

[65] By 1 March 2000 an ozone loss of about 0.8–1.8 ppmv was simulated between 425 and 490 K in accordance with observations [*Rex et al.*, 2002]. Also shown in Figure 10 is our classification of altitude ranges taken from the ClO model simulations. As would be expected, the altitude regime with the strongest ozone loss is correlated with the chlorine activation layer (I).

[66] At the top altitude (III) no significant ozone depletion is seen in the model simulations. This is likely due to the absence of PSCs in this altitude range during the winter. In the NO_x-determined layer (II) the simulated O_3 mixing ratios considerably underestimate the observed O_3 mixing ratios, because the standard simulation produces too strong a chlorine activation. Also shown is the simulated ozone loss employing an additional NO_x source as explained in section 4.1.2. In this case, the simulated O_3 mixing ratios still underestimate the observed O_3 mixing ratios by almost 0.5 ppmv, nevertheless the O_3 simulations agree best with the observations, as was found for the ClO, HCl, and NO_x mixing ratios.

[67] Using the kinetics of the ClO self-reaction by *Bloss et al.* [2001] compared to those of *Sander et al.* [2000] in our model simulations yielded only small differences in ClO mixing ratios averaging 0.1 ppbv (see Figures 4 and 5) and consequently yielded no substantial differences in the deduced ozone loss (not shown in Figure 10).

[68] If the vertical profile of ozone loss is integrated over the CH_4 range of 0.4–1.5 ppmv (corresponding to ≈110–30 hPa), 77 DU is obtained as an estimate of the loss in column ozone on 1 March 2000. Assuming an accuracy of 5% for the ozonesonde measurements in the altitude range in question yields an uncertainty of 10 DU for the deduced column ozone loss. It is difficult to compare such a single value with values reported as vortex averages or vortex core averages. However, a loss of 77 ± 10 DU on 1 March 2000 results in ≈105 DU in mid-March assuming a loss of ≈2 DU per day in early March [*Rex et al.*, 2002] a value that is in agreement with the maximum losses and also in accordance with the average ozone loss considering the common uncertainties reported for mid-March 2000 in the vortex core based on HALOE measurements [*Müller et al.*, 2002].

5. Discussion

5.1. Kinetics of the ClO Self-Reaction

[69] Our model simulations show that for 27 January 2000 measured ClO mixing ratios can best be reproduced in the model by using the kinetics of the ClO self-reaction recently reported by *Bloss et al.* [2001]. Simulated ClO mixing ratios for 1 March 2000 with either the ClO self-reaction kinetics by *Bloss et al.* [2001] or by *Sander et al.* [2000] are both within the uncertainties of the measurements. The kinetics of the ClO self-reaction by *Bloss et al.* [2001] was also found to lead to an improved agreement between ClO in situ measurements on board the HALOZ payload launched on 27 January 2000 from Kiruna 1 hour after TRIPLE and model simulations [*Vömel et al.*, 2001].

5.2. NO_x-Determined Layer

[70] In the NO_x-determined layer, low ClO mixing ratios $\ll$100 pptv were measured both on 27 January and 1 March 2000. Our ClO measurements at these altitudes agree well with ClO measurements obtained by the ClO/BrO instrument on board the HALOZ payload on 27 January, 1 March, and 8 March 2000 [*Vömel et al.*, 2001]. Simulations performed with the SLIMCAT model by A. Robinson et al. (unpublished manuscript, 2002) also overestimate the ClO mixing ratios measured at 550 K by HALOZ on 8 March 2000. Here we performed further sensitivity studies for the NO_x-determined layer which are discussed in the following.

[71] An indication that model simulations overestimate measured ClO mixing ratios at ≈22 km was reported by *Klein et al.* [2000] for January/February 1999 during the Arctic winter. [*Klein et al.*, 2000] assumed that in this winter uncertainties in UKMO temperatures [*Knudsen et al.*, 2001] could produce the discrepancies between simulated and measured ClO mixing ratios at the altitudes of interest. Uncertainties in UKMO temperatures were also reported for the winter 1999/2000; *Knudsen et al.* [2002] reported a standard deviation of UKMO temperatures ranging from 1.0–1.3 K. Single events show temperature differences between UKMO temperatures and measurements of up to ±5 K. Therefore we performed model simulations along trajectories with temperatures modified by a constant offset of −2 K, +2 K, +4 K, and +6 K. These simulations show that for 27 January 2000 assuming a temperature enhancement of approximately 4–6 K allows the low measured ClO mixing ratios to be reproduced in the model. Similar simulations for 1 March 2000 reproduce the measured ClO mixing ratios for a temperature enhancement of approximately 2–6 K. For this assumption no PSC occurrence and consequently no chlorine activation was simulated. However, satellite measurements of POAM III [*Bevilacqua et al.*, 2002] demonstrate that PSC occurred during the Arctic winter 1999/2000 at the altitudes and during the time periods considered here. Because PSC occurrence was very inhomogeneous during the Arctic winter 1999/2000, it cannot be demonstrated with certainty that in the air parcels investigated here chlorine was activated. Therefore for 1 March 2000, we checked our model results through a comparison of simulated HCl and NO_x mixing ratios with HALOE measurements. The low mixing ratios measured by HALOE demonstrate for the NO_x-determined layer that the air was activated during the winter. Thus uncertainties in UKMO temperatures and uncertainties arising from accumulated errors along the calculated trajectories could be the reason for the substantial overestimation of the observed ClO mixing ratios for 27 January 2000; although this is very unlikely for 1 March 2000.

[72] Further model studies considering the stratospheric NO_x source due to galactic cosmic rays [*Müller and Crutzen*, 1993] were performed, but the simulated ClO mixing ratios are still too large in comparison with measurements. Simulations with an alternative hypothetical NO_x source were performed to test the magnitude of such an

additional NO_x source that would be required to successfully simulate the low observed ClO mixing ratios. Transport of NO_x-rich air from the mesosphere and upper stratosphere to the lower stratosphere constitutes a NO_x source for the stratosphere; it is, however, unclear whether this NO_x source is strong enough to cause a rapid chlorine deactivation which would explain the observed low ClO values [e.g., *Callis and Lambeth*, 1998; *Jackman et al.*, 2000; *Callis et al.*, 2001]. For 1 March 2000, simulations with an additional permanent NO_x emission rate of 300–1000 [molecules cm^{-3} s^{-1}] can best reproduce the measured ClO mixing ratios as well as the NO_x mixing ratios measured by HALOE and, further, the observed ozone loss. Nonetheless, the simulated ClO mixing ratios are slightly too large and the simulated HCl and NO_x mixing ratios are somewhat too low compared to the observations. Moreover, solar proton events (SPE) are temporary sources of NO_x in the upper atmosphere. In fact, the solar maximum was reached in mid 2000 so that the sun was very active in the winter 1999/2000. For example, on 17 February 2000 two M-class solar flares erupted and were followed by a coronal mass ejection (CME) [*Wang et al.*, 2001]. Further, the NOAA Space Environment Services Center reported a weak solar proton event on 18 February 2000 (http://umbra.nascom.nasa.gov) and a strong SPE on 14–15 July 2000 [*Jackman et al.*, 2001; *Randall et al.*, 2001]. Again, none of these processes is a likely explanation for the noted discrepancy between observed and simulated ClO mixing ratios. Thus the dilemma is that for the winter 1999/2000 we cannot clearly identify a process producing additional NO_x in the lower stratosphere at a sufficiently strong rate, neither a permanent source such as galactic cosmic rays or transport processes from the mesosphere and upper stratosphere nor a temporary source such as a solar proton event (SPE).

[73] Another possibility of producing sufficient levels of NO_x would be if hydrolysis of N_2O_5 were completely suppressed. Again no such process is known. However, enhanced N_2O_5 mixing ratios were measured by the MkIV instrument on 3 December 1999 (2.9 ppbv N_2O_5 at 700–800 K, see Tables 1 and 2) and on 15 March 2000 (up to 0.9 ppbv at 500–600 K). This could also be an indication that such a process exists.

[74] These results could also indicate that the chemistry controlling the NO_y partitioning is not yet completely understood. For example, *Stowasser et al.* [2002] reported discrepancies in both NO_y observations and observed NO_y partitioning in comparison with SLIMCAT and KASIMA simulations for the Arctic winter 1998/1999 at similar altitudes as those discussed here. As in our model studies, these model simulations underestimate the observed NO_y mixing ratios so that the absence of an additional unknown NO_x source in the models could cause these discrepancies.

[75] For 1 March we assumed in our simulations that during the winter denitrification occurred in the NO_x-determined layer. The simulations show that the simulated ClO mixing ratios are very sensitive to the rate of the assumed denitrification and the magnitude of the assumed NO_x source. At these altitudes NO_y observations are only available from the MkIV instrument on 3 December 1999 and 15 March 2000 [*Popp et al.*, 2001]. *Popp et al.* [2001] derived a small denitrification for this time period and altitude range (≈2.0–4.5 ppbv NO_y at ≈525–550 K). Unfortunately, for the exact time period considered in our studies no NO_y measurements are available, therefore we cannot corroborate our assumptions on denitrification by measurements.

[76] Further, a comparison between model simulations for the NO_x-determined layer with and without denitrification shows that in simulations with denitrification no PSC formation occurred during February 1999 at the altitudes considered (see Figure 9). This is consistent with measurements by POAM III [*Bevilacqua et al.*, 2002]: POAM III observed PSCs in the altitude range between 21 and 25 km from December 1999 until the beginning of February 2000 with short interruptions at the beginning and the end of January. In the time period from mid-February to mid-March PSCs only occurred up to an altitude of 20 km. The absence of PSCs at the end of January at altitudes of the NO_x-determined layer could also be an indication that denitrification had occurred before end of January in the air masses considered, because there were PSCs before end of January and chlorine was activated, therefore the low measured ClO mixing ratios must be caused by deactivation. This indicates that uncertainties in UKMO temperatures and uncertainties arising from accumulated errors along the calculated trajectories do not cause the measured ClO mixing ratios to be low.

[77] Moreover, on 27 January 2000 TRIPLE observed chlorine activation from ≈400 K (≈16 km) to ≈575 K (≈24 km). At similar altitudes POAM III observed PSCs early in the winter (generally between 17 and 25 km). On 1 March 2000, TRIPLE observed chlorine activation from ≈400 K (≈17 km) to ≈500 K (≈21 km) and a weak chlorine activation between ≈350 and 375 K (≈13–16 km) probably caused by activation on the background aerosol. Again, POAM III observed PSCs at similar altitudes. PSCs reappear in late February and into March 2000 forming at lower altitudes between ≈13 and 20 km and centered roughly at 16 km. Summarizing the results for 1 March 2000, ClO, HCl, and NO_x mixing ratios measured by TRIPLE and by HALOE in the NO_x-determined layer can only be simulated simultaneously for a specific parameter setup assuming denitrification and an additional unidentified NO_x source.

5.3. Integration Solvers

[78] Finally, we discuss the integration solvers used in CLaMS (see section 3.1). The explicit stiff solver SVODE was used to integrate all the model simulations presented [*McKenna et al.*, 2002b]. We also compared simulations with SVODE to simulations employing the family concept (IMPACT). Significant discrepancies between simulated ClO mixing ratios were only obtained for simulations of sunset conditions. Here the relatively slow dimer (Cl_2O_2) formation controls the partitioning within the ClO_x family (= Cl + ClO + 2 × Cl_2O_2) so that ClO_x in the air parcel considered is not in chemical equilibrium. It is a precondition for applying the family concept that the family of species considered is in chemical equilibrium; therefore it was necessary to use a stiff solver for simulations presented here for sunset conditions.

6. Summary and Conclusions

[79] We presented the vertical distribution of ClO inside the Arctic polar vortex measured during daylight and

darkness on 27 January 2000 and on 1 March 2000 observed on board the TRIPLE payload and quasi-simultaneously measured ozone mixing ratios. Using CLaMS as a photochemical box model, the seasonal behavior of ClO and ozone depletion were simulated and compared with measurements for the potential temperature range of 350–620 K (≈13–25 km altitude).

[80] The seasonal variation of ClO is simulated by initializing the model in early winter on 3 December 1999 largely with data from the MkIV instrument on the OMS remote balloon payload. For both flights, simulated ClO mixing ratios show a good overall agreement with measured ClO mixing ratios within uncertainties arising from accumulated errors along air parcel histories. Model simulations indicate that the sensitivity to the surface area of the background aerosol is generally small.

[81] Model simulations performed with recently reported kinetics of the ClO self-reaction by *Bloss et al.* [2001] are compared to simulations performed with rate constants recommended by *Sander et al.* [2000]. ClO mixing ratios measured on 27 January 2000 can only be reproduced by model simulations using kinetics of the ClO self-reaction by *Bloss et al.* [2001]. Model simulations for 1 March 2000 show an agreement within the uncertainties of the ClO measurements for both reaction rate constants.

[82] Chlorine activation was observed in model simulations up to ≈575 K potential temperature (≈24 km altitude) on 27 January 2000 and up to ≈500 K potential temperature (≈21 km altitude) on 1 March 2000 consistent with PSC occurrence observed by POAM III [*Bevilacqua et al.*, 2002].

[83] Further, we found a layer of low ClO mixing ratios <100 pptv between 600 and 620 K for the flight on 27 January 2000 and between 525 and 550 K on 1 March 2000. For this layer, here referred to as NO_x-determined layer, we found substantial discrepancies between measured and simulated ClO mixing ratios. Potential causes such as uncertainties in UKMO temperatures or uncertainties arising from accumulated errors along the calculated trajectories could be excluded for 1 March 2000.

[84] Different mechanisms producing additional NO_x in the gas phase, and thus causing a more rapid chlorine deactivation, were analyzed. Although suppressing heterogeneous hydrolysis of N_2O_5 and invoking a NO_x source produced by galactic cosmic rays generally reduced simulated ClO mixing ratios, this could not reproduce the low ClO mixing ratios measured by TRIPLE. Simulations with different parameterizations of heterogeneous chemistry implemented in CLaMS also showed no substantial differences at the altitudes of interest. Only if an additional hypothetical NO_x source was implemented in CLaMS could the measured low ClO mixing ratios be approximately simulated. Such a NO_x source would have to be ≈30 times stronger than NO_x formation by galactic cosmic rays.

[85] Furthermore, for 1 March 2000 we compared HALOE measurements within the vortex with simulated HCl and NO_x mixing ratios. An overall agreement was found for all altitudes considered. For the NO_x-determined layer we have to assume both the existence of an hypothetical additional NO_x source and the occurrence of denitrification to reproduce ClO, HCl, and NO_x measured by TRIPLE and HALOE. Thus we conclude that denitrification must have occurred up to ≈550 K potential temperature (≈24 km altitude) on 1 March 2000.

[86] Model simulations and measurements show that between late January and 1 March, a substantial ozone loss was derived of about 0.8–1.8 ppmv between 425 and 490 K potential temperature correlated with the enhanced ClO mixing ratios. For 1 March 2000, if the vertical profile of ozone loss is integrated over the pressure range of ≈110–30 hPa, 77 ± 10 DU is obtained as an estimate of the loss in column ozone.

[87] Using kinetics of the ClO self-reaction by *Bloss et al.* [2001] compared to kinetics by *Sander et al.* [2000] in model simulations we found no substantial differences in the deduced ozone loss. Thus the recently reported kinetics of the ClO self-reaction by *Bloss et al.* [2001] cannot resolve the reported discrepancies between simulated and observed ozone loss in previous cold winters.

[88] **Acknowledgments.** The authors gratefully acknowledge the work performed by the teams from CNES and ESRANGE in carrying out the balloon flights and especially for the excellent implementation of the new type of flight profile, James M. Russell III (Hampton University) for providing the HALOE V19 data, and the UK Met Office (UKMO) for the meteorological analysis data. We thank S. Tilmes for analyzing the HALOE profiles. Armin Afchine, Jochen Bartels, Reimar Bauer, Erich Klein, Holger Röppischer, and Vicheith Tan are acknowledged for technical support. We thank one anonymous reviewer for the very helpful review. The experimental activities were partly funded by the European Commission, within the THESEO 2000 campaign under contract number EVK2-1999-00047 and by the German Ministry of Education and Research (BMBF). The measurements from the HALOZ gondola were supported by the U. S. National Science Foundation. The MkIV measurements were supported by NASA.

References

Abbatt, J. P. D., and M. J. Molina, Heterogeneous interactions of $ClONO_2$ and HCl on nitric acid trihydrate at 202 K, *J. Phys. Chem.*, *96*, 7674–7679, 1992.

Anderson, J. G., D. W. Toohey, and W. H. Brune, Free radicals within the Antarctic vortex: The role of CFCs in Antarctic ozone loss, *Science*, *251*, 39–46, 1991.

Austin, J., Comparison of stratospheric air parcel trajectories calculated from SSU and LIMS satellite data, *J. Geophys. Res.*, *81*, 7837–7851, 1986.

Becker, G., R. Müller, D. S. McKenna, M. Rex, and K. S. Carslaw, Ozone loss rates in the Arctic stratosphere in the winter 1991/92: Model calculations compared with Match results, *Geophys. Res. Lett.*, *25*, 4325–4328, 1998.

Becker, G., J.-U. Grooß, D. S. McKenna, and R. Müller, Stratospheric photolysis frequencies: Impact of an improved numerical solution of the radiative transfer equation, *J. Atmos. Chem.*, *37*, 217–229, 2000.

Bevilacqua, R. M., et al., Observations and analysis of polar stratospheric clouds detected by POAM III during the 1999/2000 Northern Hemisphere winter, *J. Geophys. Res.*, *107*(D20), 8281, doi:10.1029/2001JD000477, 2002.

Bloss, W. J., S. L. Nickolaisen, R. J. Salawitch, R. R. Friedl, and S. P. Sander, Kinetics of the ClO self-reaction and 210 nm absorption cross section of the ClO dimer, *J. Phys. Chem. A*, *105*, 11,226–11,239, 2001.

Brune, W. H., J. G. Anderson, and K. R. Chan, In situ observations of ClO in the Antarctic: ER-2 aircraft results from 54°S to 72°S latitude, *J. Geophys. Res.*, *94*, 16,649–16,663, 1989.

Callis, L. B., and J. D. Lambeth, NO_y formed by precipitation electron events in 1991 and 1992: Descent into the stratosphere as observed by ISAMS, *Geophys. Res. Lett.*, *25*, 1875–1878, 1998.

Callis, L. B., M. Natarajan, and J. D. Lambeth, Solar-atmospheric coupling by electrons (SOLACE): 3. Comparisons of simulations and observations, 1979–1997, issues and implications, *J. Geophys. Res.*, *106*, 7523–7539, 2001.

Carslaw, K. S., S. L. Clegg, and P. Brimblecombe, A thermodynamic model of the system HCl-HNO_3-H_2SO_4-H_2O, including solubilities of HBr, from 328 K to < 200 K, *J. Phys. Chem.*, *99*, 11,557–11,574, 1995.

Carslaw, K. S., T. Peter, and R. Müller, Uncertainties in reactive uptake coefficients for solid stratospheric particles: 2. Effect on ozone depletion, *Geophys. Res. Lett.*, *24*, 1747–1750, 1997.

Carver, G. D., and P. A. Scott, IMPACT: An implicit time integration scheme for chemical species and families, *Ann. Geophys.*, *18*, 337–346, 2000.

Carver, G. D., P. D. Brown, and O. Wild, The ASAD atmospheric chemistry integration package and chemical reaction database, *Comput. Phys. Commun.*, *105*, 197–215, 1997.

Crutzen, P. J., I. A. S. Isaksen, and G. C. Reid, Solar proton events: Stratospheric sources of nitric oxide, *Science*, *189*, 457–459, 1975.

DeMore, W. B., S. P. Sander, D. M. Goldan, R. F. Hampson, M. J. Kurylo, C. J. Howard, A. R. Ravishankara, C. E. Kolb, and M. J. Molina, Chemical kinetics and photochemical data for use in stratospheric modeling, *JPL Publ. 97-4*, 1997.

Deniel, C., R. M. Bevilacqua, J. P. Pommereau, and F. Lefèvre, Arctic chemical ozone depletion during the 1994–95 winter deduced from POAM II satellite observations and the REPROBUS three-dimensional model, *J. Geophys. Res.*, *103*, 19,231–19,244, 1998.

Deshler, T., and S. J. Oltmans, Vertical profiles of volcanic aerosol and polar stratospheric clouds above Kiruna, Sweden: Winters 1993 and 1995, *J. Atmos. Chem.*, *30*, 11–23, 1998.

Douglass, A. R., M. R. Schoeberl, R. S. Stolarski, J. W. Waters, J. M. Russell III, A. E. Roche, and S. T. Massie, Interhemispheric differences in springtime production of HCl and $ClONO_2$ in the polar vortices, *J. Geophys. Res.*, *100*, 13,967–13,978, 1995.

Drdla, K., and M. R. Schoeberl, Microphysical modeling of the 1999–2000 Arctic winter: 2. Chlorine activation and ozone depletion, *J. Geophys. Res.*, 107, 8319, doi:10.1029/2001JD001159, 2002 [printed *108*(D5), 2003].

Elkins, J. W., et al., Airborne gas chromatograph for in situ measurements of long-lived species in the upper troposphere and lower stratosphere, *Geophys. Res. Lett.*, *23*, 347–350, 1996.

Engel, A., U. Schmidt, and R. A. Stachnik, Partitioning between chlorine reservoir species deduced from observations in the Arctic winter stratosphere, *J. Atmos. Chem.*, *27*, 107–126, 1997.

Fahey, D. W., et al., The detection of large HNO_3-containing particles in the winter Arctic stratosphere, *Science*, *291*, 1026–1031, 2001.

Gidel, L. T., P. J. Crutzen, and J. Fishman, A two-dimensional photochemical model of the atmosphere: 1. Chlorocarbon emissions and their effect on stratospheric ozone, *J. Geophys. Res.*, *88*, 6622–6640, 1983.

Gordley, L. L., et al., Validation of nitric oxide and nitrogen dioxide measurements made by the halogen occultation experiment for UARS platform, *J. Geophys. Res.*, *101*, 10,240–10,266, 1996.

Goutail, F., et al., Total ozone depletion in the Arctic during the winters of 1993–94 and 1994–95, *J. Atmos. Chem.*, *32*, 35–59, 1999.

Grooß, J.-U., Modelling of stratospheric chemistry based on HALOE/UARS satellite data, Ph.D. thesis, Univ. of Mainz, Germany, 1996.

Grooß, J.-U., et al., Simulation of ozone depletion in spring 2000 with the Chemical Lagrangian Model of the Stratosphere (CLaMS), *J. Geophys. Res.*, *107*(D20), 8295, doi:10.1029/2001JD000456, 2002.

Hansen, G., T. Svenøe, M. P. Chipperfield, A. Dahlback, and U.-P. Hoppe, Evidence of substantial ozone depletion in winter 1995/96 over Northern Norway, *Geophys. Res. Lett.*, *24*, 799–802, 1997.

Hanson, D. R., and A. R. Ravishankara, Reaction of $ClONO_2$ with HCl on NAT, NAD, and frozen sulfuric acid and hydrolysis of N_2O_5 and $ClONO_2$ on frozen sulfuric acid, *J. Geophys. Res.*, *98*, 22,931–22,936, 1993.

Harris, N., R. Hudson, and C. Phillips (Eds.), Assessment of trends in the vertical distribution of ozone, in *SPARC Rep. 1*, World Meteorol. Org., Geneva, 1998.

Heaps, M. G., Parametization of the cosmic ray ion-pair production rate above 18 km, *Planet. Space Sci.*, *26*, 513–517, 1978.

Jackman, C. H., E. L. Fleming, and F. M. Vitt, Influence of extremely large solar proton events in a changing stratosphere, *J. Geophys. Res.*, *105*, 11,659–11,670, 2000.

Jackman, C. H., R. D. McPeters, G. J. Labow, E. L. Fleming, C. J. Praderas, and J. M. Russell, Northern Hemisphere atmospheric effects due to the July 2000 solar proton event, *Geophys. Res. Lett.*, *28*, 2883–2886, 2001.

Kilbane-Dawe, I., N. Harris, J. Pyle, M. Rex, A. Lee, and M. Chipperfield, A comparison of Match and 3D model ozone loss rates in the Arctic polar vortex during the winters of 1994/95 and 1995/96, *J. Atmos. Chem.*, *39*, 123–138, 2001.

Klein, U., K. Lindner, I. Wohltmann, and K. F. Künzi, Winter and spring observations of stratospheric chlorine monoxide from Ny-Ålesund, Spitzbergen, in 1997/98 and 1998/99, *Geophys. Res. Lett.*, *27*, 4093–4096, 2000.

Knudsen, B. M., J.-P. Pommereau, A. Garnier, M. Nunez-Pinharanda, L. Denis, G. Letrenne, M. Durand, and J. M. Rosen, Comparison of stratospheric air parcel trajectories based on different meterological analysis, *J. Geophys. Res.*, *106*, 3415–3424, 2001.

Knudsen, B. M., J.-P. Pommereau, A. Garnier, M. Nunes-Pinharanda, L. Denis, P. Newman, G. Letrenne, and M. Durand, Accuracy of analyzed stratospheric temperatures in the winter Arctic vortex from infrared Montgolfier long-duration balloon flights: 2. Results, *J. Geophys. Res.*, *107*(D20), 4316, doi:10.1029/2001JD001329, 2002.

Konopka, P., J. U. Grooß, G. Günther, D. S. McKenna, R. Müller, J. W. Elkins, D. Fahey, and P. Popp, Weak impact of mixing on chlorine deactivation during SOLVE/THESEO 2000: Lagrangian modeling (CLaMS) versus ER-2 in situ observations, *J. Geophys. Res.*, *108*(D5), 8324, doi:10.1029/2001JD000876, 2003.

Larsen, N., et al., Microphysical mesoscale simulations of polar stratospheric cloud formation constrained by in situ measurements of chemical and optical cloud properties, *J. Geophys. Res.*, *107*(D20), 8301, doi:10.1029/2001JD000999, 2002.

Lary, D. J., and J. A. Pyle, Diffuse radiation, twilight, and photochemistry - I, *J. Atmos. Chem.*, *13*, 373–406, 1991.

Levin, I., H. Glatzel-Mattheier, T. Marik, M. Cuntz, M. Schmidt, and D. Worthy, Verification of German methane emission inventories and their recent changes based on atmospheric observations, *J. Geophys. Res.*, *104*, 3447–3456, 1999.

Manney, G. L., and J. L. Sabutis, Development of the polar vortex in the 1999–2000 Arctic winter stratosphere, *Geophys. Res. Lett.*, *27*, 2589–2592, 2000.

McKenna, D. S., J.-U. Grooß, G. Günther, P. Konopka, R. Müller, G. Carver, and Y. Sasano, A new Chemical Lagrangian Model of the Stratosphere (CLaMS): 2. Formulation of chemistry scheme and initialization, *J. Geophys. Res.*, *107*(D15), 4256, doi:10.1029/2000JD000113, 2002a.

McKenna, D. S., P. Konopka, J.-U. Grooß, G. Günther, R. Müller, R. Spang, D. Offermann, and Y. Orsolini, A new Chemical Lagrangian Model of the Stratosphere (CLaMS) 1. Formulation of advection and mixing, *J. Geophys. Res.*, *107*(D16), 4309, doi:10.1029/2000JD000114, 2002b.

Müller, R., and P. J. Crutzen, A possible role of galactic cosmic rays in chlorine activation during polar night, *J. Geophys. Res.*, *98*, 20,483–20,490, 1993.

Müller, R., et al., Chlorine activation and chemical ozone loss deduced from HALOE and balloon measurements in the Arctic during the winter of 1999–2000, *J. Geophys. Res.*, 107, 8302, doi:10.1029/2001JD001423, 2002 [printed *108*(D5), 2003].

Neher, H. V., Cosmic-ray knee in 1958, *J. Geophys. Res.*, *66*, 4007–4012, 1961.

Neher, H. V., Cosmic-ray particles that changed from 1954 to 1958 to 1965, *J. Geophys. Res.*, *72*, 1527–1539, 1967.

Neher, H. V., Cosmic-rays at high latitudes and altitudes covering four solar maxima, *J. Geophys. Res.*, *76*, 1637–1651, 1971.

Newman, P. A., et al., An overview of the SOLVE/THESEO 2000 campaign, *J. Geophys. Res.*, *107*(D20), 8259, doi:10.1029/2001JD001303, 2002.

Pierson, J. M., K. A. McKinney, D. W. Toohey, J. Margitan, U. Schmidt, A. Engel, and P. A. Newman, An investigation of ClO photochemistry in the chemically perturbed Arctic vortex, *J. Atmos. Chem.*, *32*, 61–81, 1999.

Popp, P. J., et al., Severe and extensive denitrification in the 1999–2000 Arctic winter stratosphere, *Geophys. Res. Lett.*, *28*, 2875–2878, 2001.

Randall, C. E., D. E. Siskind, and R. M. Bevilacqua, Stratospheric NO_x enhancements in the Southern Hemisphere vortex in winter/spring of 2000, *Geophys. Res. Lett.*, *28*, 2385–2388, 2001.

Ray, E. A., F. L. Moore, J. W. Elkins, D. F. Hurst, P. A. Romashkin, G. S. Dutton, and D. W. Fahey, Descent and mixing in the 1999–2000 northern polar vortex inferred from in situ tracer measurements, *J. Geophys. Res.*, *107*(D20), 8285, doi:10.1029/2001JD000961, 2002.

Rex, M., et al., Chemical depletion of Arctic ozone in winter 1999/2000, *J. Geophys. Res.*, *107*(D20), 8276, doi:10.1029/2001JD000533, 2002.

Russell, J. M., L. L. Gordley, J. H. Park, S. R. Drayson, A. F. Tuck, J. E. Harries, R. J. Cicerone, P. J. Crutzen, and J. E. Frederick, The Halogen Occultation Experiment, *J. Geophys. Res.*, *98*, 10,777–10,797, 1993.

Salawitch, R. J., et al., Chemical loss of ozone during the Arctic winter of 1999/2000: An analysis based on balloonborne observations, *J. Geophys. Res.*, *107*(D20), 8269, doi:10.1029/2001JD000620, 2002.

Sander, S. P., et al., Chemical kinetics and photochemical data for use in stratospheric modeling, Supplement to evaluation 12: Update of key reactions, *JPL Publ. 00-3*, 2000.

Schiller, C., et al., Dehydration in the artic stratosphere during the SOLVE/THESEO-2000 campaigns, *J. Geophys. Res*, *107*(D20), 8293, doi:10.1029/2001JD000463, 2002.

Schmidt, U., G. Kulessa, E. Klein, E.-P. Röth, P. Fabian, and R. Borchers, Intercomparison of balloon-borne cryogenic whole air samplers during the MAP/GLOBUS 1983 campaign, *Planet. Space Sci.*, *35*, 647–656, 1987.

Schmidt, U., R. Bauer, A. Engel, R. Borchers, and J. Lee, The variation of available chlorine Cl_y in the Arctic polar vortex during EASOE, *Geophys. Res. Lett.*, *21*, 1215–1218, 1994.

Schreiner, J., et al., Chemical, microphysical, and optical properties of polar stratospheric clouds, *J. Geophys. Res.*, 107, 8313, doi:10.1029/2001JD000825, 2002 [printed *108*(D5), 2003].

Sinnhuber, B.-M., et al., Large loss of total ozone during the Arctic winter of 1999/2000, *Geophys. Res. Lett.*, *27*, 3473–3476, 2000.

Solomon, S., Progress towards a quantitative understanding of Antarctic ozone depletion, *Nature*, *347*, 347–354, 1990.

Stowasser, M., et al., A characterization of the warm 1999 Arctic winter by observations and modeling: NO_y partitioning and dynamics, *J. Geophys. Res.*, *107*(D19), 4376, doi:10.1029/2001JD001217, 2002.

Toohey, D. W., L. M. Avallone, N. T. Allen, J. N. Demusz, J. N. Hazen, N. L. Hazen, and J. G. Anderson, The performance of a new instrument for in situ measurements of ClO in the lower stratosphere, *Geophys. Res. Lett.*, *20*, 1791–1794, 1993.

Toon, G. C., et al., Comparison of MkIV balloon and ER-2 aircraft measurements of atmospheric trace gases, *J. Geophys. Res.*, *104*, 26,779–26,790, 1999.

Voigt, C., et al., Nitric acid trihydrate (NAT) in polar stratospheric clouds, *Science*, *290*, 1756–1758, 2000.

Vömel, H., D. Toohey, T. Deshler, and C. Kröger, Sunset observations of ClO in the arctic polar vortex and implications for ozone loss rates, *Geophys. Res. Lett.*, *28*, 4183–4186, 2001.

Wang, H., J. Chae, V. Yurchyshyn, G. Yang, M. Steinegger, and P. Goode, Inter-active region connection of sympathetic flaring on 2000 February 17, *Astrophys. J.*, *559*, 1171–1179, 2001.

Woyke, T., R. Müller, F. Stroh, D. S. McKenna, A. Engel, J. J. Margitan, M. Rex, and K. S. Carslaw, A test of our understanding of the ozone chemistry in the Arctic polar vortex based on in situ measurements of ClO, BrO, and O_3 in the 1994/95 winter, *J. Geophys. Res.*, *104*, 18,755–18,768, 1999.

Wu, J., and A. E. Dessler, Comparisons between measurements and models of Antarctic ozone loss, *J. Geophys. Res.*, *106*, 3195–3202, 2001.

Zhang, R., J. T. Jayne, and M. J. Molina, Heterogeneous interactions of $ClONO_2$ and HCl with sulfuric acid tetrahydrate: Implications for the stratosphere, *J. Phys. Chem.*, *98*, 867–874, 1994.

Zhong, W., and J. D. Haigh, Improved broadband emissivity parameterization for water vapor cooling rate calculations, *J. Atmos. Sci.*, *52*(1), 124–138, 1995.

T. Deshler, Department of Atmospheric Science, University of Wyoming, Laramie, WY 82071, USA. (deshler@uwyo.edu)

J.-U. Grooß, R. Müller, F. Stroh, and B. Vogel, Institut für Stratosphärische Chemie (ICG-I), Forschungszentrum Jülich, D-52425 Jülich, Germany. (j.-u.grooss@fz-juelich.de; ro.mueller@fz-juelich.de; f.stroh@fz-juelich.de; b.vogel@fz-juelich.de)

J. Karhu, Finnish Meteorological Institute, FIN-99600 Sodankylä, Finland. (juha.karhu@fmi.fi)

D. S. McKenna, National Center for Atmospheric Research, 1850 Table Mesa Drive, Boulder, CO 80307-3000, USA. (danny@acd.ucar.edu)

M. Müller, Institut für Meteorologie und Geophysik, Johann Wolfgang Goethe Universität, Georg Voigt Strasse 14, D-60325 Frankfurt, Germany. (m.mueller@meteor.uni-frankfurt.de)

D. Toohey, Program in Atmospheric and Oceanic Sciences, University of Colorado, Boulder, CO 80309-0311, USA. (toohey@colorado.edu)

G. C. Toon, Jet Propulsion Laboratory, Mail-Stop 183-601, 4800 Oak Grove Drive, Pasadena, CA 91109, USA. (geoffrey.c.toon@jpl.nasa.gov)